Defense Nuclear Agency
Alexandria, VA 22310-3398

DNA-TR-94-178

MATVENT – A Simple Model for Blast Venting from a Responding Chamber

Dev S. Srinivasa
Logicon R/D Associates
P.O. Box 92500
Los Angeles, CA 90009

May 1996

Technical Report

CONTRACT No. DNA 001-93-C-0138

DISCLAIMER NOTICE

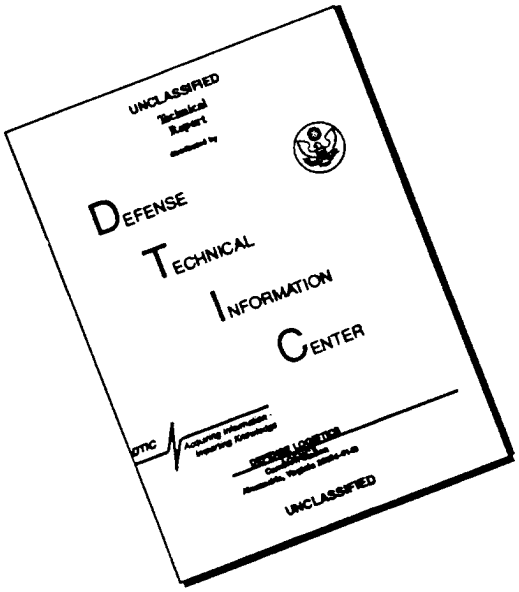

THIS DOCUMENT IS BEST QUALITY AVAILABLE. THE COPY FURNISHED TO DTIC CONTAINED A SIGNIFICANT NUMBER OF PAGES WHICH DO NOT REPRODUCE LEGIBLY.

Destroy this report when it is no longer needed. Do not return to sender.

PLEASE NOTIFY THE DEFENSE NUCLEAR AGENCY, ATTN: CSTI, 6801 TELEGRAPH ROAD, ALEXANDRIA, VA 22310-3398, IF YOUR ADDRESS IS INCORRECT, IF YOU WISH IT DELETED FROM THE DISTRIBUTION LIST, OR IF THE ADDRESSEE IS NO LONGER EMPLOYED BY YOUR ORGANIZATION.

DISTRIBUTION LIST UPDATE

This mailer is provided to enable DNA to maintain current distribution lists for reports. (We would appreciate your providing the requested information.)

☐ Add the individual listed to your distribution list.

☐ Delete the cited organization/individual.

☐ Change of address.

NOTE:
Please return the mailing label from the document so that any additions, changes, corrections or deletions can be made easily. For distribution cancellation or more information call DNA/IMAS (703) 325-1036.

NAME: _____

ORGANIZATION: _____

OLD ADDRESS	CURRENT ADDRESS
_____	_____
_____	_____
_____	_____

TELEPHONE NUMBER: ( ) _____

DNA PUBLICATION NUMBER/TITLE	CHANGES/DELETIONS/ADDITIONS, etc.) *(Attach Sheet if more Space is Required)*
_____	_____
_____	_____
_____	_____

DNA OR OTHER GOVERNMENT CONTRACT NUMBER: _____

CERTIFICATION OF NEED-TO-KNOW BY GOVERNMENT SPONSOR (if other than DNA):

SPONSORING ORGANIZATION: _____

CONTRACTING OFFICER OR REPRESENTATIVE: _____

SIGNATURE: _____

CUT HERE AND RETURN

DEFENSE NUCLEAR AGENCY
ATTN: IMAS
6801 TELEGRAPH ROAD
ALEXANDRIA, VA 22310-3398

DEFENSE NUCLEAR AGENCY
ATTN: IMAS
6801 TELEGRAPH ROAD
ALEXANDRIA, VA 22310-3398

REPORT DOCUMENTATION PAGE

Form Approved
OMB No. 0704-0188

1. AGENCY USE ONLY (Leave blank)	2. REPORT DATE	3. REPORT TYPE AND DATES COVERED
	960501	Technical 930301 - 940131

4. TITLE AND SUBTITLE
MATVENT – A Simple Model for Blast Venting from a Responding Champer

5. FUNDING NUMBERS
C - DNA 001-93-C-0138
PE - 62715H
PR - AB
TA - KA
WU - DH310900

6. AUTHOR(S)
Dev S. Srinivasa

7. PERFORMING ORGANIZATION NAME(S) AND ADDRESS(ES)
Logicon R/D Associates
P.O. Box 92500
Los Angeles, CA 90009

8. PERFORMING ORGANIZATION REPORT NUMBER
RDA-TR-211-4261-3101-001

9. SPONSORING/MONITORING AGENCY NAME(S) AND ADDRESS(ES)
Defense Nuclear Agency
6801 Telegraph Road
Alexandria, VA 22310-3398
SPWE/Myers

10. SPONSORING/MONITORING AGENCY REPORT NUMBER
DNA-TR-94-178

11. SUPPLEMENTARY NOTES
This work was sponsored by the Defense Nuclear Agency under RDT&E RMC Code B4662D AB KA EA011 1110A 25904D.

12a. DISTRIBUTION/AVAILABILITY STATEMENT
Approved for public release; distribution is unlimited.

12b. DISTRIBUTION CODE

13. ABSTRACT *(Maximum 200 words)*

A simple PC-based model MATVENT for the calculation of venting from a responding chamber is described. The venting source is assumed to be blast-fluidized material in the chamber. Approximate treatments of mechanical and/or thermal response of the chamber walls and materials to the internal blast are incorporated into a quasi-steady treatment of fluid mechanics in the chamber. The model is coded in the MATLAB language (a registered trademark of the MathWorks, Inc., Natick, MA) and allows rapid trade-off studies for experiment design. Parametric calculations with MATVENT produce time histories of the fluid mechanical variables of interest in the chamber as well as histories of the mass flow rate, vented mass and, where needed, the relative volume change of the chamber and/or relative heat loss to the chamber walls. Two important quantities, namely, venting durations and total vented masses also can be obtained. A recent experiment is modeled in a set of parametric calculations with MATVENT and the results are presented. The results indicate that in small scale experiments with low blast yields, the selection of the chamber material and the thermal characteristics of the chamber wall surfaces can significantly affect the amount of vented mass. The results also show that the venting durations and vented masses are not yield-scaleable if responding chambers are employed in experiments. The model is capable of extension to simulate venting from multiple interconnected chambers in one of which an explosion might be set off, and of accommodating more sophisticated response models.

14. SUBJECT TERMS
Blast Venting
Internal Blast
Efflux Velocity
Collateral Effect
Chemical/Biological Effects

16. PRICE CODE
92

15. NUMBER OF PAGES

17. SECURITY CLASSIFICATION OF REPORT	18. SECURITY CLASSIFICATION OF THIS PAGE	19. SECURITY CLASSIFICATION OF ABSTRACT	20. LIMITATION OF ABSTRACT
UNCLASSIFIED	UNCLASSIFIED	UNCLASSIFIED	SAR

NSN 7540-280-5500

Standard Form 298 (rev. 2-89)
Prescribed by ANSI Sta. 239-298-102

CLASSIFIED BY:

N/A since Unclassified.

DECLASSIFY ON:

N/A since Unclassified.

PREFACE

The author is grateful to Mr. T.A. Mazzola for analyzing the available experimental data and providing overpressure impulse comparison points used in this report, and also for the many helpful discussions, general support and encouragement.

The author thanks Dr. Gary Ganong of Logicon RDA for providing information and data from "Expulsion Experiment No. 1" conducted at the U.S. Army Waterways Experiment Station, Vicksburg, Mississippi, and other useful discussions.

The author is also grateful to Major John W. Kyme of DNA/SPWE for the sponsorship and encouragement provided during the course of the work reported here, and to Major D. Myers of DNA/SPWE for reviewing the report.

The computer program MATVENT described in this report is written in the MATLAB language, a registered trademark of The MathWorks, Inc., Natick, MA 01760. MATVENT is not a registered trademark. The Office of the Secretary of Defense (OSD) has not validated the program MATVENT.

CONVERSION TABLE

Conversion factors for U.S. Customary to metric (SI) units of measurement

MULTIPLY ----------→ BY ----------→TO GET
TO GET ←---------- BY ←---------- DIVIDE

atmosphere(normal)	1.013 25 X E +2	kilo pascal (kPa)
bar	1.000 000 X E +2	kilo pasacal (kPa)
Btu (thermochemical)	1.054 350 X E +3	joule (J)
Btu (thermochemical)/h.ft.°F	1.729 577	joules/s.m .°K
Btu (thermochemical)/s.ft^2.°F	2.042 808 X E+4	joules/s.m^2.°K
Btu (thermochemical)/lb.°F	4.184 000 X E+3	joules/kg.°K
calorie (thermochemical)	4.184 000	jolule (J)
cal (thermochemical)/cm^2	4.184 000 X E -2	mega joule/m^2 (MJ/m^2)
degree Fahrenheit	t°K = (t°F+459.67)/1.8	degree Kelvin (K)
erg	1.000 000 X E -7	joule (J)
erg/second	1.000 000 X E -7	watt (W)
foot	3.048 000 X E -1	meter (m)
foot-pound-force	1.355 818	joule (J)
gallon (U.S. liquid)	3.785 412 X E -3	meter^3 (m^3)
inch	2.540 000 X E -2	meter (m)
kilotons	4.183	terajoules
micron	1.000 000 X E -6	meter (m)
pound-force/inch^2 (psi)	6.894 747	kilo pascal (kPa)
pound-mass (lbm avoirdupois)	4.535 924 X E -1	kilogram (kg)
pound-mass/foot^3	1.601 846 X E +1	kilogram/meter^3 (kg/m^3)
slug	1.459 390 X E +1	kilogram (kg)

TABLE OF CONTENTS

TABLE OF CONTENTS (Continued)

FIGURES

SECTION 1
INTRODUCTION

1.1 BACKGROUND.

There has been renewed interest in explosions inside chambers with vents for both safety and military reasons. Escape of hazardous vented materials is of great concern in ensuring civilian safety; it is also quite important in estimating collateral effects from military operations against stored chemical/biological agents. The effects of internal blast on the venting of material contained within is currently not fully understood. As such, more experiments are being conducted to understand venting from internal blast and new predictive models are being developed. In designing blast-venting experiments, there appears to be a need for a simple model for rapid trade-off studies that combines the effects of fluid mechanics, thermal and mechanical factors on venting. In this report, a blast venting model for a single chamber is described.

1.2 SCOPE OF THE REPORT.

This report documents a venting model embodied in a computer code named MATVENT, and several calculations carried out using the code to learn about the relative importance of various factors which could affect venting; of particular interest are the duration of venting and the total mass vented. The model considers the venting of gases from a blast inside a single, mechanically and thermally responding chamber with a small opening to the ambient atmosphere (Figure 1-1). "Mechanically Responding" means that the interior walls of the chamber respond to chamber pressure. "Thermally responding" refers to the change in the energetics and mechanics of venting because of the loss of blast energy through the walls by thermal effects such as conduction and convection; thermal response also includes the volume changes brought about because of thermal expansion or contraction of the walls.

The essentials of the MATVENT venting model are detailed in Section 2, along with a list of the needed input data and other assumptions. Section 3 gives a brief description of the code and the high-level language MATLAB in which the code is written. Section 4 describes the results from several parametric MATVENT calculations employing the same geometry and explosion yield as a recent experiment, briefly described in Section 4.1. For the same explosive yield, chamber contents and chamber/vent dimensions, the effects on venting of:

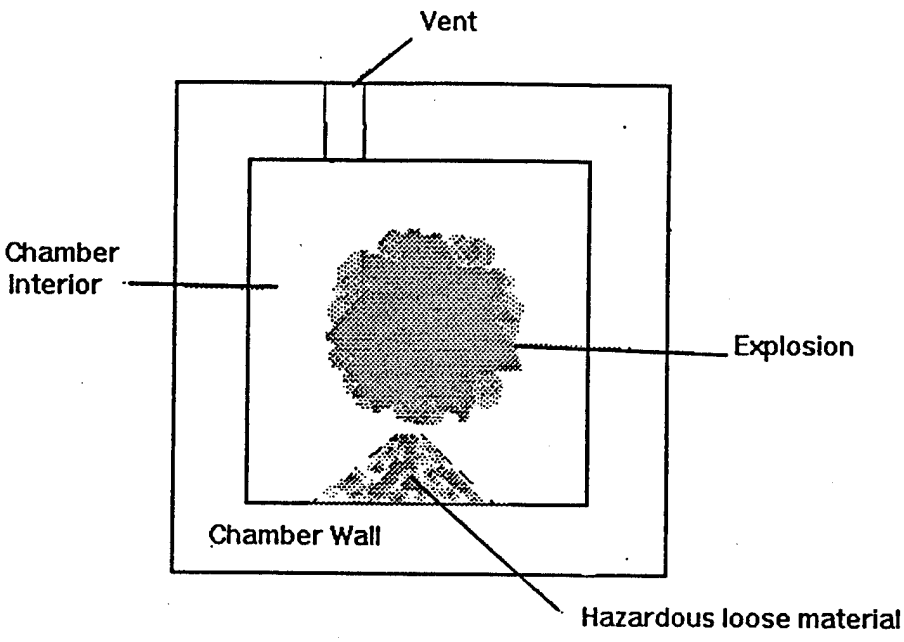

Figure 1-1. Schematic for the blast venting problem.

- assuming different specific heat ratios γ
- assuming different fluidized mass fractions of the chamber contents in a rigid and insulated chamber. The term "fluidized" refers to the "dense -gas" analytic approximation which treats the mass of loose solid material as if it were a gas uniformly distributed over the volume, intimately mixed and in equilibrium with the chamber air and explosion gases.
- assuming a chamber which is insulated but deformable
- assuming a chamber which loses energy by thermal conduction only, but does not respond to pressure
- assuming a chamber which loses energy by convection and conduction effects, without responding to pressure, and
- assuming a chamber which is fully responsive to both pressure and thermal effects,

are investigated parametrically with the objective of recognizing the relative importance of the assumptions in venting estimates. Additional calculations to resolve the applicability of yield-scaling, important in the design of scaled experiments, are reported. The effect of each set of assumptions on the important quantities, such as venting rates, total vented mass, and total venting time are obtained numerically. Section 5 discusses the calculational results and the limitations. Section 6 summarizes the results and provides recommendations for further work to improve the model. Appendix A provides the model equations which have been coded in MATVENT. In Appendix B, a listing of the basic MATVENT code is provided along with the results of a run from an example case. Finally, Appendix C provides definitions for the symbols used in the body of the report.

SECTION 2
DESCRIPTION OF THE MODEL

This section provides descriptions of the elements of the basic version of the MATVENT model as well as modifications for parametric studies. The input data needs, the fluid mechanics model element, the mechanical response element and the thermal response element are detailed.

2.1 INPUT DATA NEEDS AND OTHER ASSUMPTIONS.

The parameters needed as inputs to the model and assumed as given, are the following:

(a) The thermal and mechanical properties of the material out of which the chamber is built (steel, concrete, etc.);

(b) The convective heat transfer coefficient 'u' (also referred to sometimes as "unit surface conductance");

(c) The volume and linear dimensions of the chamber;

(d) The cross-sectional area of the vent;

(e) The mass of loose material contained within the chamber;

(f) The mass of explosive, and the effective yield of the explosive per unit mass;

(g) The fraction f of loose material fluidized by the explosion; and

(h) The specific heats and specific heat ratio (γ) of the chamber gases subsequent to the explosion.

2.2 MODEL FOR THE FLUID MECHANICS OF VENTING.

The model assumes the fluid mechanical process inside the chamber to be quasi-static and governed by the adiabatic relations for a calorically and thermally perfect ("dense") gas, as is usually done (Reference 1) for flow out of a reservoir with a vent. The model does not treat the initial shock reverberation period which might last for a very short time (of the order of tens of milliseconds) compared to total venting durations. Time zero in MATVENT can be shifted if need be to a time marking the end of the initial shock reverberation interval. The shock reverberation interval is typically a few shock transit times across a representative linear dimension of the chamber, such as the hydraulic mean diameter.

Isentropic relations applicable under the quasi-static assumption enable the calculation of the time-dependent chamber pressure, temperature and density, as well as the vented fluidized mass and venting duration, in terms of the initial conditions obtained by distributing the energy of the explosion and the mass of fluidized material uniformly over the volume of the chamber. The equations and other details of fluid mechanical modeling are given in Appendix A.

2.3 CHAMBER RESPONSE.

The modeling for mechanical and thermal response assumes that the time scale for fluid mechanical equilibration is much smaller than those for mechanical or thermal response. Even where this assumption is not quite valid, the model will still provide a "feel" for the effects of such response on the venting, and thus help orient experiment design.

2.3.1 Mechanical Response Model.

The mechanical response of the chamber to the explosion inside is modeled in the following simple manner. At each timestep δt of the calculation, the incremental overpressure impulse $p \cdot \delta t$ is obtained and divided by the specific acoustic impedance w of the wall material to obtain an incremental displacement. The volume change increment δV is the product of the total wall area AR_0 and the incremental displacement. The total volume change at any time is the sum of the incremental volume changes up to that time. Thermal expansion can, as described in Section 2.3.2, also be included at each timestep, leading to a thermal modification (reduction) of the purely mechanical incremental volume change. The updated volume at any time is obtained by adding the volume change during a timestep to the volume at the beginning of the timestep ("old volume". The density and pressure inside the chamber are adjusted using the ratio of the updated and "old" volumes. The temperature ratio is also adjusted to an updated value. The equations describing modeling for mechanical response are detailed in Appendix A.

2.3.2 Thermal Response Models.

Thermal response was initially modeled as if conduction alone were important. Later a model, presumed more realistic, was developed to take both convection near the walls as well as conduction through the walls into account.

2.3.2.1 Thermal Response Model For Conduction Alone. In modeling the thermal response alone, first a model for heat loss by conduction only was formulated. In this "conduction only" model, an "effective" penetration thickness '$\sqrt{a \cdot t}$' for the heat pulse was calculated based on the thermal diffusivity a of the chamber material and the time after blast t. This "effective thickness" is a fictitious thickness of the wall which, for the purpose of heat loss calculation only, is assumed to rise instantaneously to the applied (time-dependent) chamber temperature. The total heat loss Q to the chamber walls at time t is the product of the penetration thickness, the wall surface area, the density, the heat capacity and the chamber temperature in excess of ambient:

$$Q = -\rho_w \cdot AR_0 \cdot \sqrt{a} \cdot \sqrt{t} \cdot C \cdot (T_g - T_{0a}) \tag{2.1}$$

By differentiating the expression for heat loss at any time, the incremental heat loss δQ over the timestep δt can be obtained:

$$\delta Q = -\rho_w \cdot AR_0 \cdot \sqrt{a} \cdot C \cdot \left[\frac{1}{2\sqrt{t}}(T_g - T_{0a}) + \sqrt{t}\dot{T}_g\right] \cdot \delta t \tag{2.2}$$

The heat loss increment δQ can be expressed in terms of the chamber pressure ratio $x_g(t)$ and its time derivative $\dot{x}_g(t)$:

$$\delta Q = -\rho_w \cdot AR_0 \cdot \sqrt{a} \cdot \sqrt{t} \cdot C \cdot T_{0a} \cdot \left[\frac{1}{2 \cdot t}\left(x_g^{\frac{\gamma-1}{\gamma}} - 1\right) + \frac{\gamma - 1}{\gamma}\sqrt{t} \cdot \dot{x}_g \cdot x_g^{-\frac{1}{\gamma}}\right]\delta t \tag{2.3}$$

The net heat loss up to any time is the sum of the incremental losses over the timesteps; the net heat loss divided by the mass of the fluidized material in the chamber and the specific heat of the "dense" gas results in the change (decrease) of the chamber temperature due to conduction only. The modified chamber temperature is then used to calculate modified pressure and density, now adjusted for heat loss. The calculation proceeds until there is pressure equilibration between the chamber and the ambient air and there is no more efflux. The chamber temperature generally remains higher than the ambient at this point, while the density is lower. Details of the modeling for thermal response due to conduction only are given in Appendix A. A version of MATVENT was run for the case of thermal response due to conduction only in order to obtain a sense of how venting might be affected by conduction alone. However, thermal response by both convection and conduction, as in Section 2.3.2.2 was deemed more realistic and is included in the code listing, Appendix B, rather than response by conduction only.

2.3.2.2 Thermal Response Model For Convection and Conduction. The temperature of the wall surface in contact with the chamber gases is in practicality, not the same as the chamber interior temperature. A drop in the gas temperature in a thin layer adjacent to the wall, from the interior chamber temperature T_g to the temperature of the wall surface T_w exists in general, due to convection in the chamber. A simple model for heat loss by both convection and conduction was therefore developed in order to account for both the thermal resistance at the chamber walls and the heat conduction in the body of the chamber material. This appears to be a more realistic approach to modeling. In this model, the "effective" thickness of the chamber was assumed to rise to a temperature lower than the chamber temperature at any given time. The temperature of the "effective" thickness was calculated from a modified Newtonian heat loss equation where the heat transfer rate across the surface layer adjacent to the wall is in balance with the rate of (time-dependent) heat gain by the effective thickness (Reference 2):

$$\dot{Q} = \rho_w \cdot AR_0 \cdot \sqrt{a} \cdot \sqrt{t} \cdot C \cdot \dot{T}_w = u \cdot AR_0 \cdot (T_g - T_w) \tag{2.4}$$

Solving the above differential equation with the initial condition $T_w = T_{0a}$ at $t = 0$ (and noting that the chamber temperature T_g is to be regarded as invariant in keeping with the quasi-static assumption for the chamber conditions) leads to the wall temperature T_w at time t and the heat loss increment δQ over a timestep δt as:

$$\begin{aligned} T_w - T_{0a} &= (T_g - T_{0a}) \cdot \left(1 - \epsilon^{-2\xi\sqrt{t}}\right) \\ \delta Q &= -u \cdot AR_0 (T_g - T_{0a}) \cdot \epsilon^{-2\xi\sqrt{t}} \cdot \delta t \end{aligned} \tag{2.5}$$

The net heat loss up to any time is calculated as the sum of the incremental losses over the elapsed timesteps. The rest of the procedure follows as in the previous Section 2.3.2.1.

The volume decrease produced in the chamber purely due to thermal expansion of the "effective" thickness can be formulated as follows:

$$\begin{aligned} \delta V_{te} &= -AR_0 \cdot \epsilon \cdot \sqrt{a} \cdot \sqrt{t} \cdot (T_w - T_{0a}) \cdot \delta t \\ &= -AR_0 \cdot \epsilon \cdot \sqrt{a} \cdot \sqrt{t} \cdot (T_g - T_{0a}) \cdot \left(1 - e^{-2\xi\sqrt{t}}\right) \cdot \delta t \end{aligned} \tag{2.6}$$

The equations in the modeling for thermal response by both convection and conduction are detailed in Appendix A.

2.3.3 Combined Response Model.

Both mechanical and thermal responses can simultaneously be taken into account in the "full response" model as given in Appendices A and B.

2.4 PARAMETRIC MODELING.

The basic model assumes a constant ratio of specific heats γ; parametric calculations with different values for γ can be conducted using a modified version of the code, where the input for γ is expressed as a vector rather than as a scalar, to study the sensitivity of venting to changes in the specific heat ratio. Similarly, other parametric calculations with variations in fluidized mass fraction f, wall impedance 'w', heat diffusivity 'a', convection coefficient 'u', and yield 'W' may be performed with appropriately modified versions of the code to obtain sensitivities, to variations in each quantity, of the total vented mass, the rate at which such venting might occur and the duration of such venting.

SECTION 3
THE MATVENT CODE

The computer code embodying the venting model for responding or non-responding chambers has been named MATVENT since the code was written in the high-level language called MATLAB 4.0 (Reference 3). MATLAB ("MATrix LABoratory") is an interactive system whose basic data element is a matrix. MATLAB provides an easy-to-use computing environment for high-performance numeric computation and visualization where problems and solutions can be expressed just as they are written mathematically, without traditional programming. Particularly noteworthy with MATLAB is the ease and rapidity of generating a variety of two and three dimensional graphics. MATLAB allows the importing and exporting of programs written in other languages such as FORTRAN and C.

A listing of the basic version of the MATVENT code, embodied in a script file (called an M- file in MATLAB), named **matvent.m** is provided in Appendix B. Several versions of the code were generated and used in the calculations reported here, one version for each parametric case. No attempt at optimizing the code(s) have been made. Further optimization may result in a more compact code

MATVENT is an interactive code for use on a PC platform, preferably a 486-PC or better. The user is prompted for inputs pertaining to the chamber dimensions, wall material properties, vent area, explosive mass and yield, hazardous material (or simulant) mass and fluidized fraction, specific heats and the specific heat ratio of chamber gases, the initial and final times for the calculation, the error tolerance for the calculation and an option to see the progress of the calculation on the computer screen. Then the code calculates and sets up initializations and matrix or vector arrays for solution variables. The pressure variable at the beginning of a timestep is updated on an interim basis by using a Runge-Kutta-Fehlberg integration scheme and calling a function M-file called **intair.m** which contains expressions for the time derivative of chamber pressure. Choking is allowed for when proper. It may be mentioned in passing here that this scheme lends itself to convenient extension in problems of venting from multiple connected chambers. The chamber volume is updated by including changes over a timestep due to thermal expansion and interim pressure; the temperature decrement during the timestep due to heat loss by convection and conduction is then calculated and a new interim temperature is obtained. The final pressure, density and temperature at the end of a timestep are (re)-calculated from the isentropic relations to account for the changes in volume and temperature during

the timestep. From the final values of pressure, density, and temperature, the solution variable histories - for overpressure, overpressure impulse, density, temperature, efflux velocity, efflux Mach number, efflux mass flow rate, integrated efflux mass, relative volume change (as a percentage of original volume) and relative heat loss (as a percentage of the original blast energy) - are obtained and recorded in vector arrays (or in matrix arrays in multiple case input versions of MATVENT). In addition, if the final time is sufficient to allow pressure equilibration between the chamber and the ambient atmosphere, the venting duration and the total mass vented during the episode are also determined.

Finally, the time histories of the solution variables are plotted on the screen, annotated interactively with legends containing the important input information, and then hard copies of the plots are obtained on a printer. An example problem and its solution are included with the code listing.

MATVENT calculates the solutions swiftly, in a matter of tens of seconds to a few minutes on a 486-PC. Therefore, it is suited for rapid trade-off calculations to identify needed design features of a venting experiment. Further detailed information on a selected design may be obtained through hydrocode calculations.

SECTION 4
RESULTS OF CALCULATIONS

4.1 SIMULATED VENTING EXPERIMENTS AT WES.

A set of seven MATVENT calculations was performed for the following cases, simulating the input parameters of "Expulsion Experiment No. 1" done recently at the Waterways Experiment Station, U.S. Army Corps of Engineers (Reference 4). The rectangular solid chamber in this experiment had the internal dimensions 174.00cms x 130.81cms x 49.53cms, was made of thick ($\geq$ 5.08 cms) steel plate, and had a volume of 1.127 cubic meters. The vent area was 31.67 sq.cms. The blast was produced by a C-4 charge of mass 431 gms (0.95 lbs.) Glass beads and other loose material with a total mass of 16,116 gms were placed on the floor of the chamber, part of which were fluidized in the explosion.

4.2 MATERIAL PROPERTIES ASSUMPTIONS.

It was assumed in the calculations that the C-4 explosive released 1400 calories per gram in the explosion (Reference 5). The chamber walls, made of steel, were assumed to have the following properties (Reference 6):

- density – 7.86 gms/cc,
- acoustic speed (compressional waves) – 5,943 m/sec,
- heat conductivity – 1 J/cm · sec °K,
- heat capacity – 0.449 J/gm · °K,
- coefficient of linear expansion – 0.00001206/ °K, and
- thermal diffusivity – 0.2834 cm^2/sec.

For air, the reference properties assumed were:

- density – 0.001225 gm/cc at 298.15 °K,
- ambient pressure – 1 atmosphere (14.7 psi), and
- specific heat at constant pressure – 1.03 J/gm °K.

Heat transfer between the internal gas and the walls was governed by:

- convective heat transfer coefficient – 1.4192 J/sec · cm^2 °K

4.3 CALCULATIONAL RESULTS.

Results of the set of calculations are shown in Figures 4-1 through Figure 4-12. The calculational results show histories of overpressure ratio (i.e., chamber pressure in excess of ambient, divided by the ambient pressure), overpressure impulse ratio (overpressure ratio integrated over time), density ratio (density divided by ambient density), temperature ratio (temperature divided by ambient temperature), efflux velocity, efflux Mach number, mass flow rate, total mass of efflux, and where appropriate, relative volume change (i.e. volume change at any time divided by original chamber volume) and/or relative heat loss (i.e. heat energy lost to the walls divided by the explosion energy). The duration of venting and the total mass vented are also shown for variations of the particular parameter of each set.

4.3.1 Effects of Varying γ; Non-Responding Chamber.

Figures 4-1 and 4-2 show the effects of varying γ for the case of a rigid, insulated chamber with the assumption that two-thirds of the mass of beads was fluidized. The available experimental data from "Expulsion Experiment No. 1" are also plotted for comparison. The overpressure ratio (Figure 4-1a) and overpressure impulse ratio (Figure 4-1b) comparisons with the experiment show very poor agreement over the entire range of γ. A value of 1.35 for γ produces an initial overpressure closest to the experimental overpressure. Therefore, $\gamma = 1.35$ is the adopted standard for the rest of the parametric study.

Figure 4-1c demonstrates that the common initial value of the chamber gas density decreases at progressively slower rates in time as the assumed value for γ is decreased, so that at the end of a venting episode, lower assumed values for γ result in higher residual densities in the chamber. The chamber temperatures in Figure 4-1d, show a similar behavior except that the initial temperatures are higher with the larger values for γ. The values for efflux velocities at any time, Figure 4-1e are generally greater for larger γ but taper off rapidly towards the end of venting. Figure 4-1f shows that the duration of choked flow from the vent is reduced for $\gamma < 1.2$. Figure 4-1g indicates that the efflux mass flow rates up to approximately half of the total vent time increase with γ, but at later times, approach common values regardless of γ. The total vented mass up to any time, shown in Figure 4-1h increases with γ. Figure 4-1h shows that the total efflux mass decreases (moderately) as γ decreases from 1.4 to 1.1. Figure 4-2a shows that the venting duration is not a strong function of γ. However, Figure 4-2b indicates that the total vented mass

increases moderately as γ is increased.

4.3.2 Effects of Varying the Fluidized Mass Fraction; Non-Responding Chamber.

Figures 4-3 and 4-4 show the influence of varying the fluidized mass fraction, f, in a non-responding chamber. The mass fractions used were 2/3, 1/3, 1/10, 1/20 and 0; thus, there was a progression from two-thirds of the loose material being fluidized to only air plus the mass of the explosive. As f is increased, increases are shown at any time in the chamber overpressure (Figure 4-3a), the overpressure impulse (Figure 4-3b), the density (Figure 4-3c), the duration of choked flow (Figure 4-3f), the efflux mass flow rate (Figure 4-3g), the total efflux mass (Figure 4-3h), the total duration of venting (Figure 4-4a), and the total amount of vented mass (Figure 4-4b). The temperature decreases with increasing f (Figure 4-3d). The efflux velocity (Figure 4-3e) shows lower but longer lasting values with increases in f. Overpressure and overpressure-impulse comparisons with data from "Expulsion Experiment No. 1" are still poor for any mass fraction f.

4.3.3 Effects of Varying the Wall Impedance; Thermally Non-Responding Chamber.

Figures 4-5 and 4-6 show the effects of varying the characteristic acoustic impedance, 'w' of the wall material for a thermally non-responding chamber with the fluidized mass fraction assumed as $f = 2/3$. The impedance was varied from that of steel, w, to 0.1w. Starting with the same initial values for each quantity, the decay rates of overpressure (Figure 4-5a), density (Figure 4-5c), temperature (Figure 4-5d) and mass flow rate (Figure 4-5g) increase moderately as the impedance is decreased substantially. Figure 4-5b indicates that the overpressure impulse is higher with higher wall impedance. Figure 4-5e demonstrates that the efflux velocity history is not strongly dependent on wall impedance. Figure 4-5f shows that the duration of choked flow decreases moderately with decrease in impedance. Figure 4-5h shows that the total efflux mass decreases with decreasing wall impedance although the variation is not large. The venting duration decreases with increasing impedance (Figure 4-6a), whereas the total vented mass increases (Figure 4-6b). The relative volume change of the chamber (defined as change in volume divided by the original volume), Figure 4-5i, can be quite large as the impedance is decreased. While Fig 4-5i shows the relative volume change going from 14 to 96 percent as the impedance is decreased by a factor of ten, it has to be borne in mind that non-linear effects, not included in the current analysis, will moderate very large deformations to lower values. Comparisons with experimental overpressure and overpressure impulse data are still poor (Figures 4-5a and 4-5b).

4.3.4 Thermal Response By Conduction Only; Mechanically Non-Responding Chamber.

Figure 4-7 demonstrates the effects of assuming that the chamber, although mechanically non-responding, responds by thermal conduction and also expansion due to heating. The fluidization fraction assumed here is $f = 2/3$. The thermal diffusivities employed were 1, 1/4, 1/16, 1/100 and 0 times the value for steel, a. The results show a large effect of thermal response on the overpressure (Figure 4-7a), overpressure impulse (Figure 4-7b), density (Figure 4-7c), temperature (Figure 4-7d), efflux velocity (Figure 4-7e), mass flow rate (Figure 4-7g), and total efflux mass (Figure 4-7h), which decrease greatly as the diffusivity is increased from 0 to a. Choking durations (Figure 4-7f), as well as venting durations and total vented mass are also greatly affected by increases in diffusivity from 0 to a. The overpressure and overpressure impulse data from "Expulsion Experiment No. 1" fall within a band between 0.01a and 0.0625a, and follow the trends reasonably well; however, since that range of diffusivities is unrealistic for steel, it is believed that conduction alone cannot account for energy losses due to heat transfer. A slight volume decrease of the chamber due to thermal expansion and a large amount of heat loss to the walls are indicated by Figures. 4-7i and 4-7j, respectively.

4.3.5 Thermal Response By Convection and Conduction; Mechanically Non-Responding Chamber.

Results shown in Figure 4-8 assume that the heat loss is due to both conduction and convection. The chamber is assumed to be mechanically non-responding. The coefficients of convection employed were 0, u/10, u/4, u/2 and u, where u = 1.42 J/sec $\cdot$ cm^2 $\cdot$ °K; the fluidization fraction assumed is $f = 2/3$. The plots for time histories of overpressure (Figure 4-8a), overpressure impulse (Figure 4-8b), density (Figure 4-8c), temperature (Figure 4-8d), efflux velocity (Figure 4-8e), mass flow rate (Figure 4-8g), and total efflux mass (Figure 4-8h) show substantial decreases in those quantities when the assumed convection coefficient is increased in value. Choking flow durations (Figure 4-8f) also show a decrease with increase of convection coefficient. The relative volume change, due to thermal expansion only (Figure 4-8i) appears to be of minor significance, whereas the increase in relative heat loss (Figure 4-8j) with increasing convection coefficient can be quite large ($> 40\%$ for the nominal case with u = 1.42 J/sec $\cdot$ cm^2 $\cdot$ °K). In particular, the plots show again that the total efflux mass is a strong function of thermal response, with the efflux mass decreasing significantly as the convection coefficient is increased. For the nominal

value of 1.42 J/sec · cm^2 °K, the overpressure and overpressure impulse comparisons with experiment, Figures 4-8a and 4-8b, are quite good. The total efflux mass for this case, Figure 4-8h, is 889 gms, and the bead mass vented will be 761 gms (i.e., f x 889 gms), which may be compared to a mass loss of 1081 gms (which might be an upper bound since it included vaporized material and escaped dust of unknown amount, Reference 7) in the experiment.

4.3.6 Fully Responding Chamber.

Figures 4-9 and 4-10 show the results for a chamber which responds both mechanically and thermally. It is assumed here also that the fluidization fraction $f = 2/3$. The convection coefficient was varied from u to zero as in case 4.3.5. The results show the same trends as case 4.3.5. With the convection coefficient assumed to have the nominal value u, the overpressure ratio (Figure 4-9a) and overpressure impulse ratio (Figure 4-9b) compare well with experiment. The final value of the overpressure impulse (0.65 psi-sec) is slightly lower than that for case 4.3.5 (0.678 psi-sec); similarly the total efflux mass (865 gms) is also somewhat lower than in case 4.3.5 (889 gms). The total efflux mass for the fluidized beads is 741 gms on a proportional basis (i.e., f x 865 gms) which is consistent with the experimental data. The total venting time (Figure 4-10a) and the total vented mass (Figure 4-10b) decrease, as in case 4.3.5, as the convection coefficient is increased. The relative volume change (which includes both mechanical and thermal components), Figure 4-9i, is seen to be in the range between one percent for the highest value u of the convection coefficient to 14% for u = 0. The relative heat loss, Figure 4-9j, is seen to range from 53% for the case with convection coefficient u to 0 for a thermally non-responding case (u = 0).

4.3.7 Scaling Issues.

Figures 4-11 and 4-12 depict the results obtained when different yields and corresponding "yield-scaled" chambers and chamber contents are assumed. These calculations employed a fluidized fraction $f = 2/3$, thermal diffusivity a = 0.2834 cm^2/sec, convection coefficient u = 1.42 J/sec · cm^2 · °K, and wall impedance w = $4 \cdot 67 \cdot 10^6$ gm/cm^2 · sec. The parametric yields used were multiples of 1, 8, 64, 343, and 1,000 times the 431 gms of C-4 used in the WES "Expulsion Experiment No. 1". Corresponding chamber volumes, explosive masses and hazardous material masses also had the same multiples. Vent areas were 2/3 power multiples while linear dimensions were 1/3 power multiples. The solution variables were also appropriately scaled. Time in each case was scaled by the inverse 1/3 power of the yield multiple. If yield scaling is valid, a single curve should represent the time history

of any particular solution variable on a scaled basis for all yields. This does not appear to be the case since in a responding chamber, the losses of energy due to mechanical and thermal processes do not scale with yield. In general, the yield-scaled venting duration and total mass vented increase as the yield increases, as shown by Figures 4-12a and 4-12b, respectively.

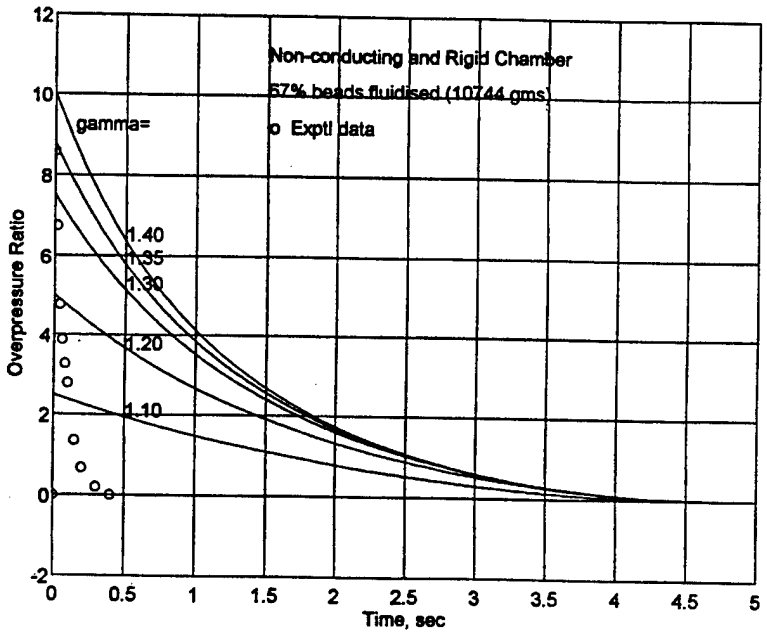

a.) Overpressure ratio history.

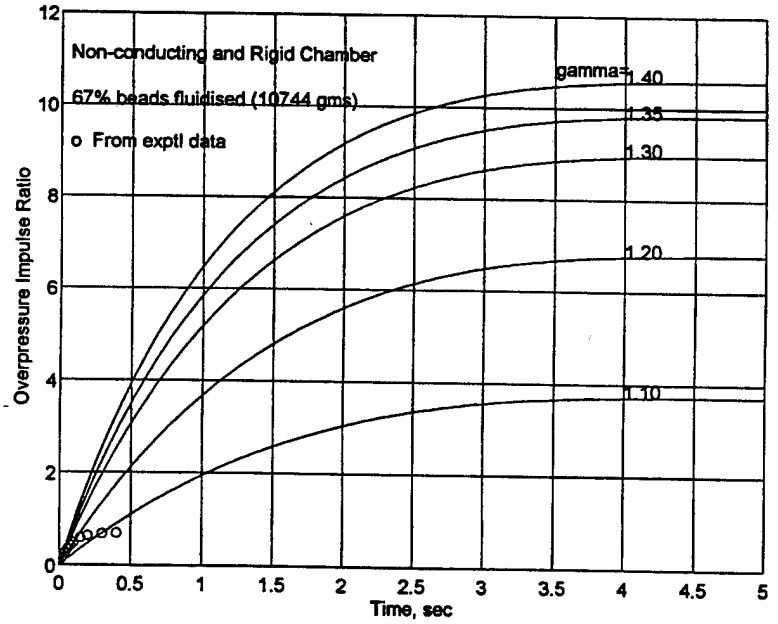

b.) Overpressure impulse ratio history.

Figure 4-1. Blast venting — effect of varying gamma.

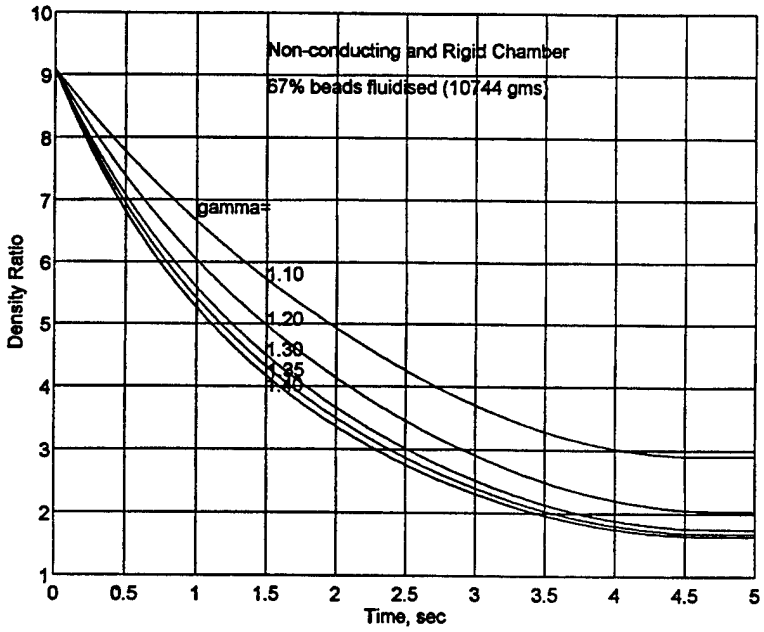

c.) Density ratio history.

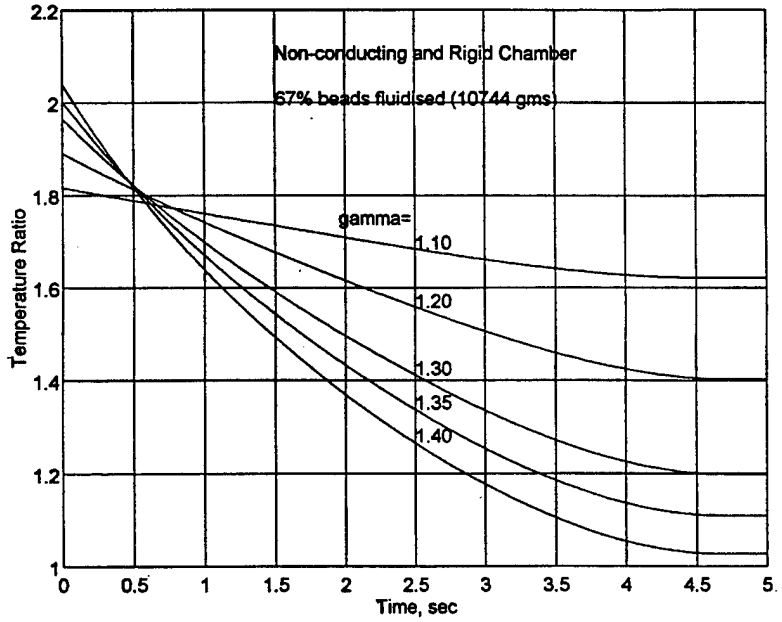

d.) Temperature ratio history.

Figure 4-1. Blast venting — effect of varying gamma (Continued).

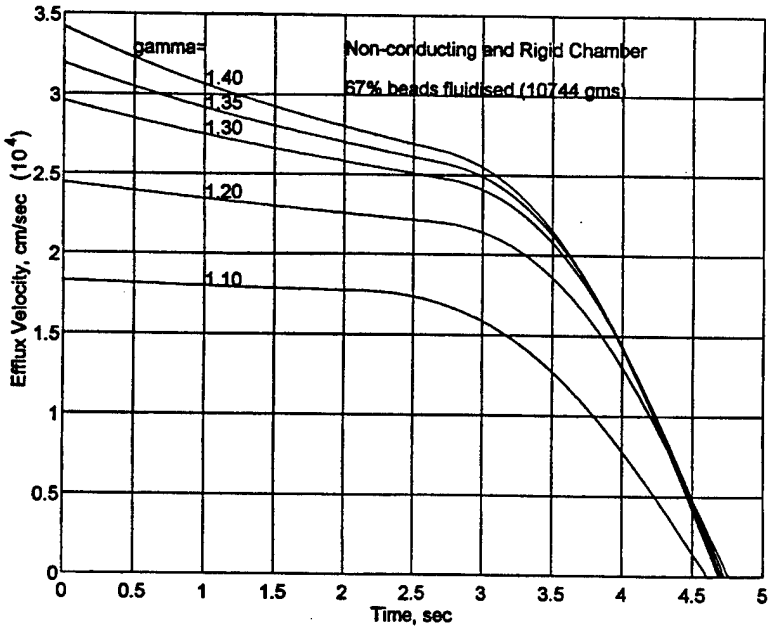

e.) Efflux velocity history.

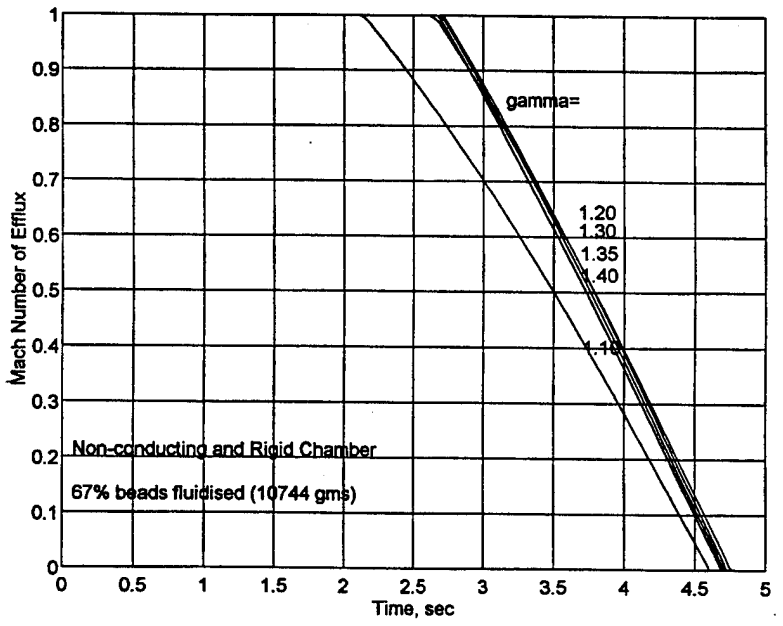

f.) Mach number history.

Figure 4-1. Blast venting — effect of varying gamma (Continued).

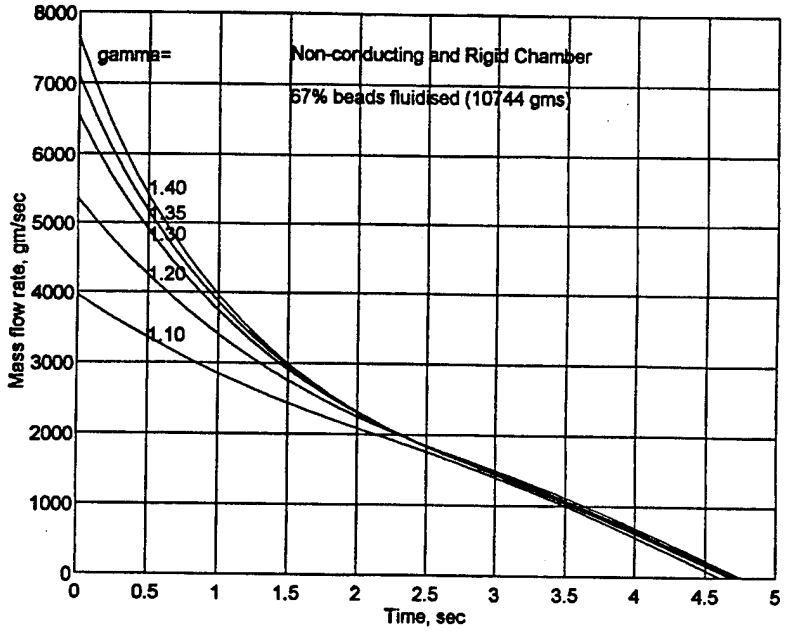

g.) Mass flow rate history.

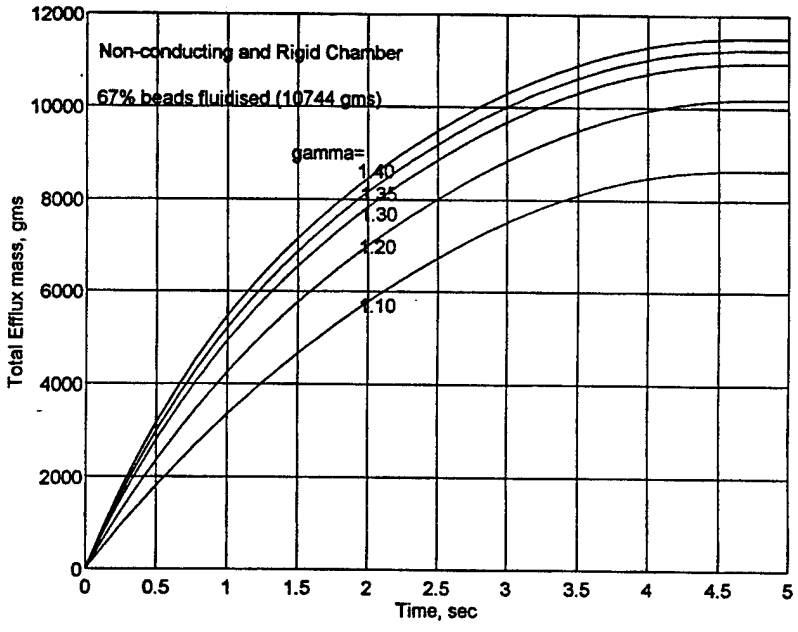

h.) Total efflux mass history.

Figure 4-1. Blast venting — effect of varying gamma (Continued).

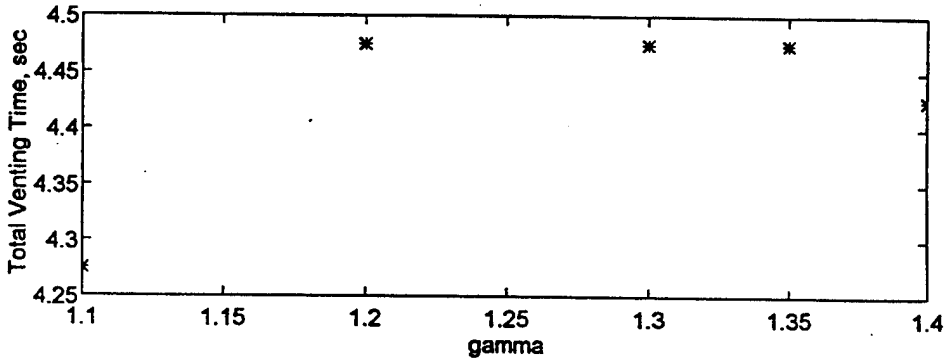

a.) Total venting time.

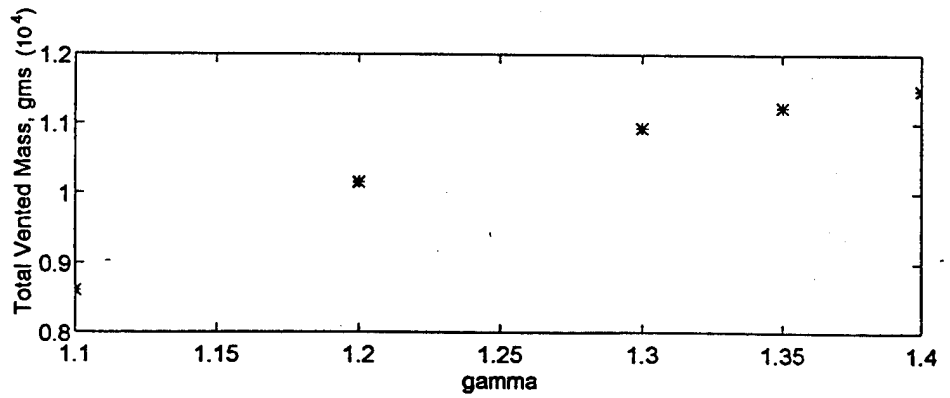

b.) Total vented mass.

Figure 4-2. Dependence of vent duration and vented mass on gamma.

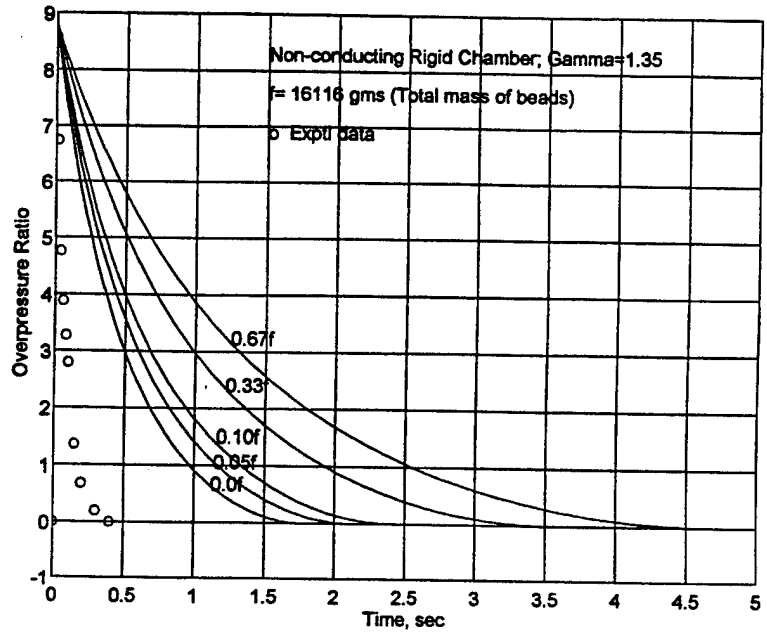

a.) Overpressure ratio history.

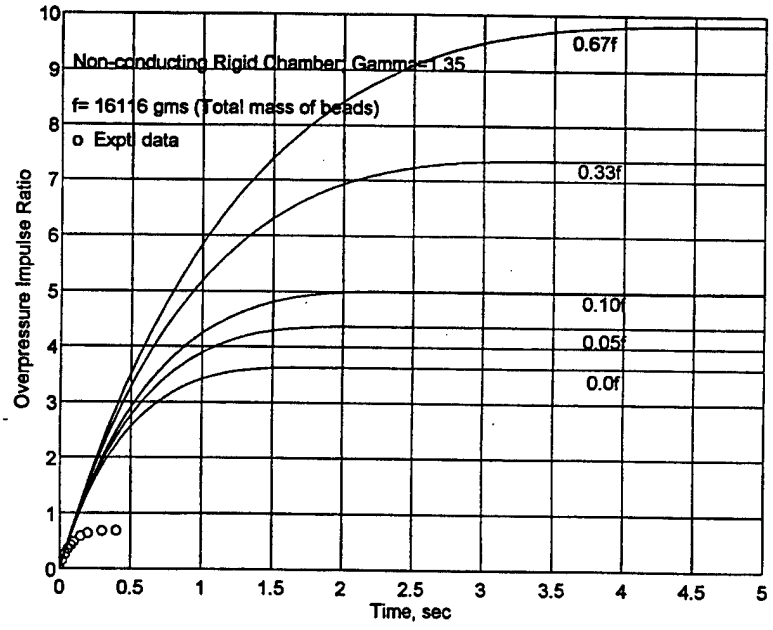

b.) Overpressure impulse ratio history.

Figure 4-3. Blast venting — effect of mass loading.

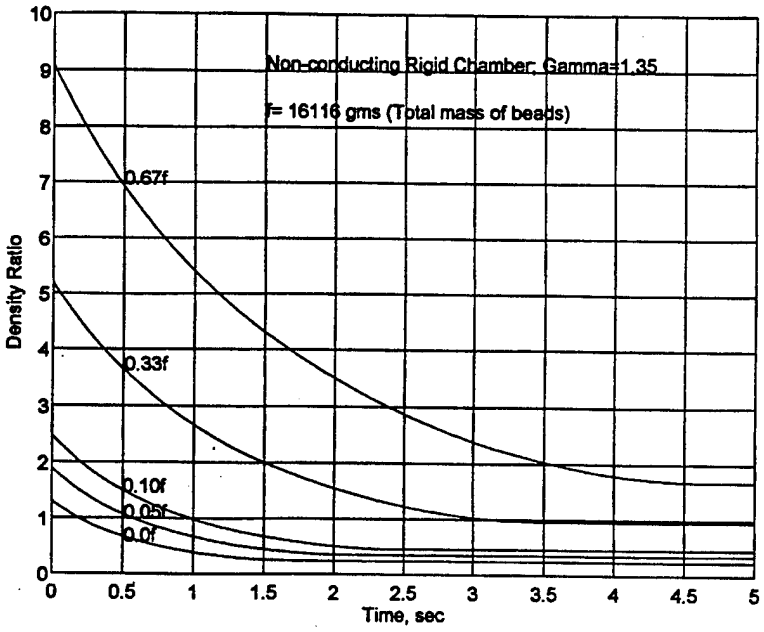

c.) Density ratio history.

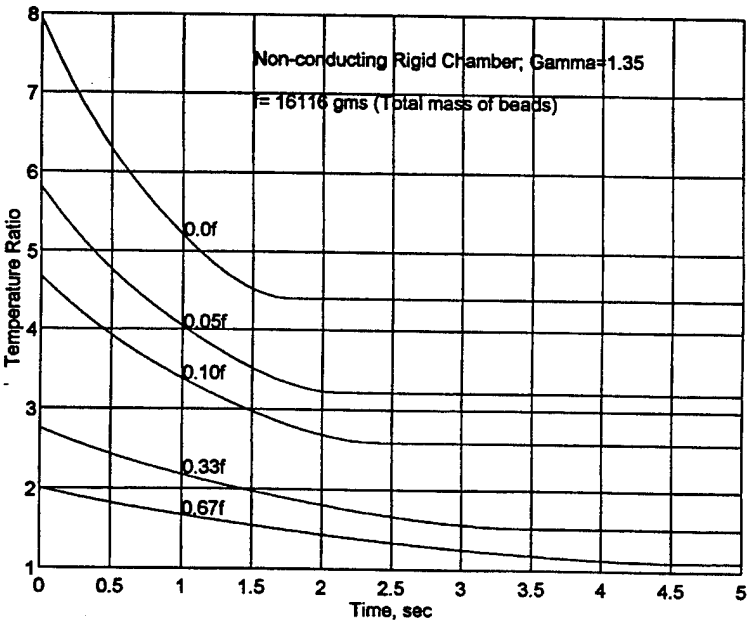

d.) Temperature ratio history.

Figure 4-3. Blast venting — effect of mass loading (Continued).

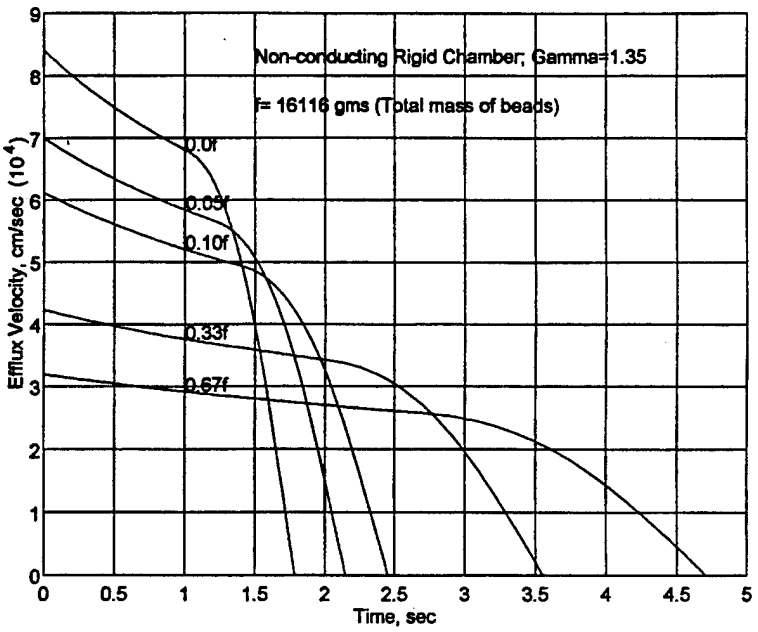

e.) Efflux velocity history.

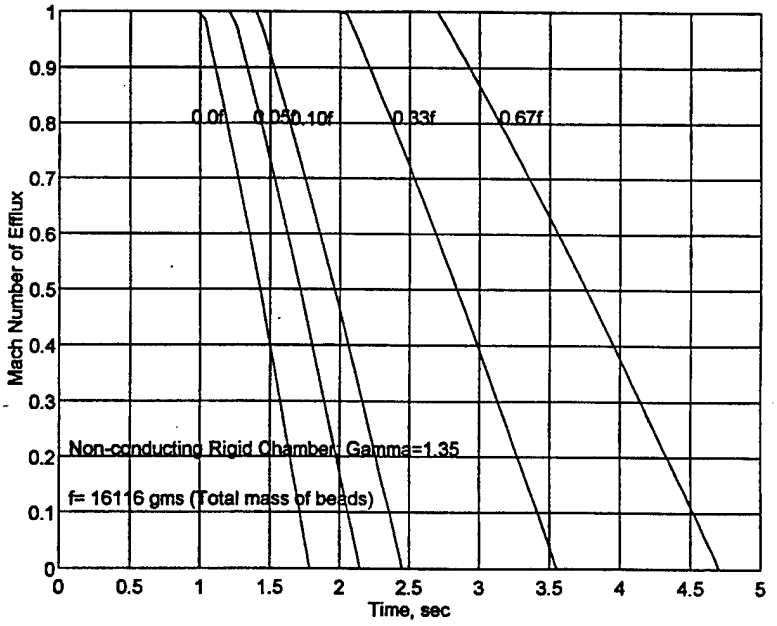

f.) Mach number history.

Figure 4-3. Blast venting — effect of mass loading (Continued).

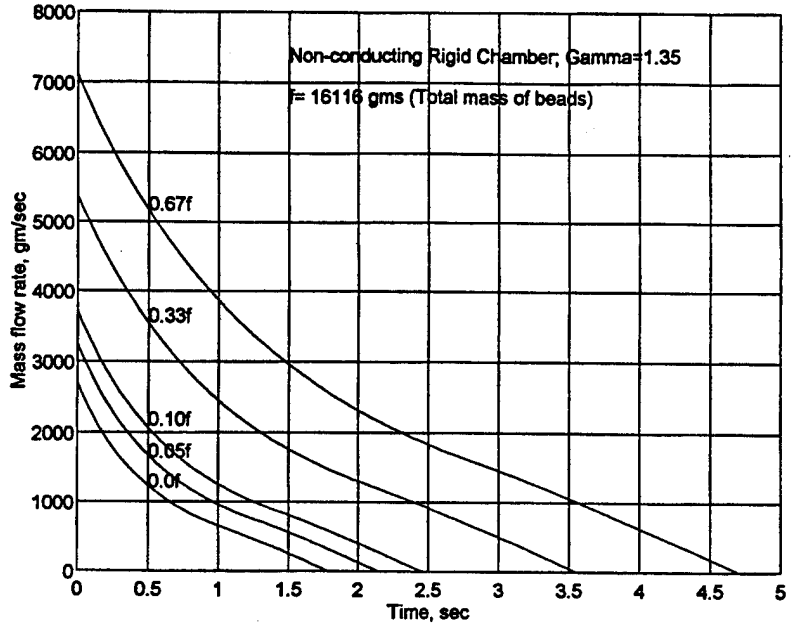

g.) Mass flow rate history.

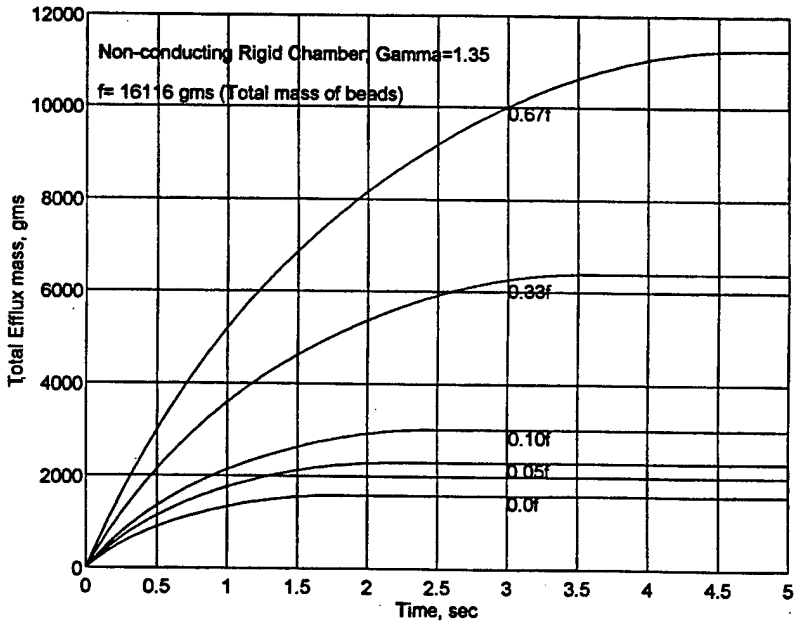

h.) Total efflux mass history.

Figure 4-3. Blast venting — effect of mass loading (Continued).

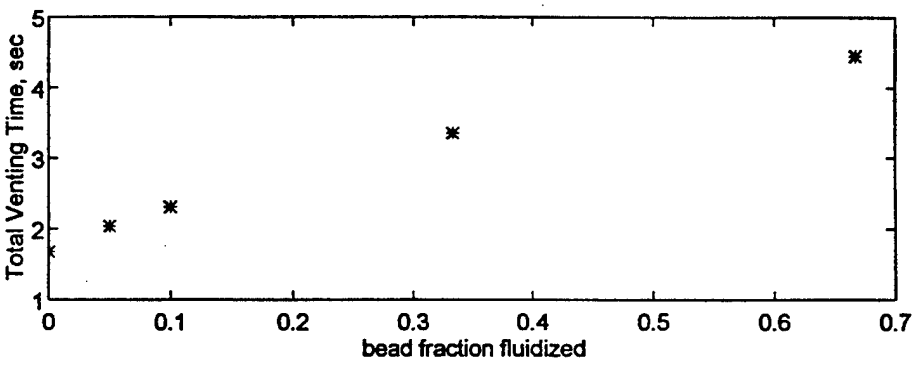

a.) Total venting time.

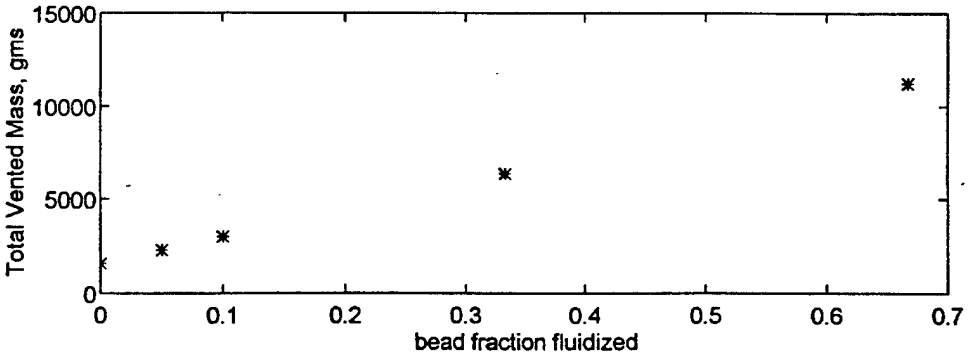

b.) Total vented mass.

Figure 4-4. Dependence of vent duration and vented mass on fluidized bead fraction.

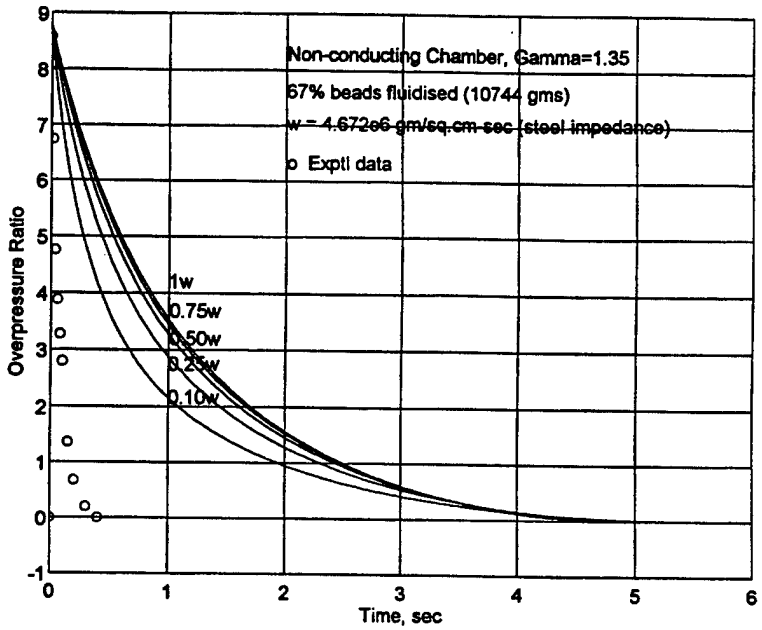

a.) Overpressure ratio history.

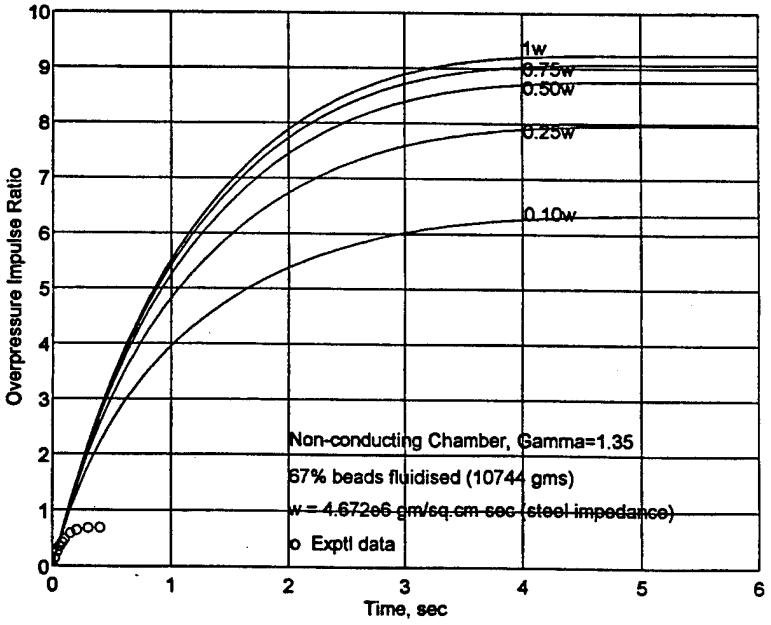

b.) Overpressure impulse ratio history.

Figure 4-5. Blast venting — effect of wall compliance.

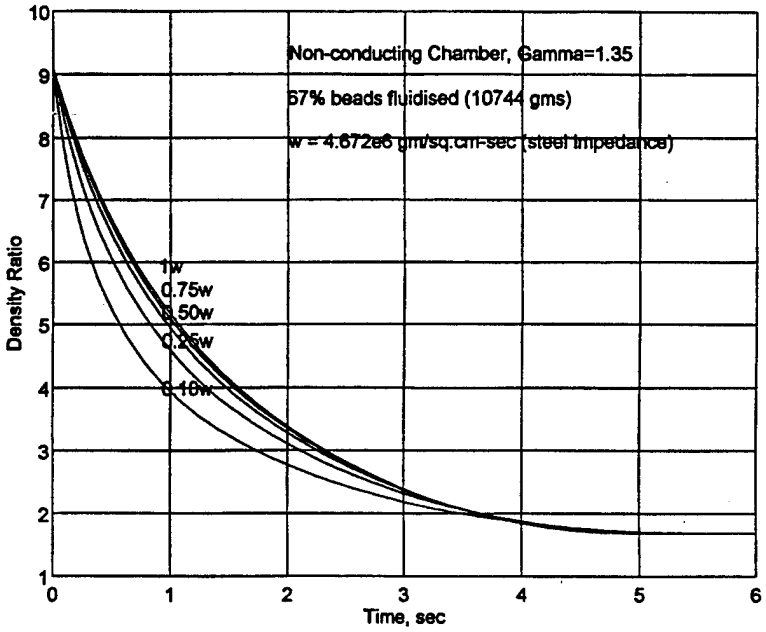

c.) Density ratio history.

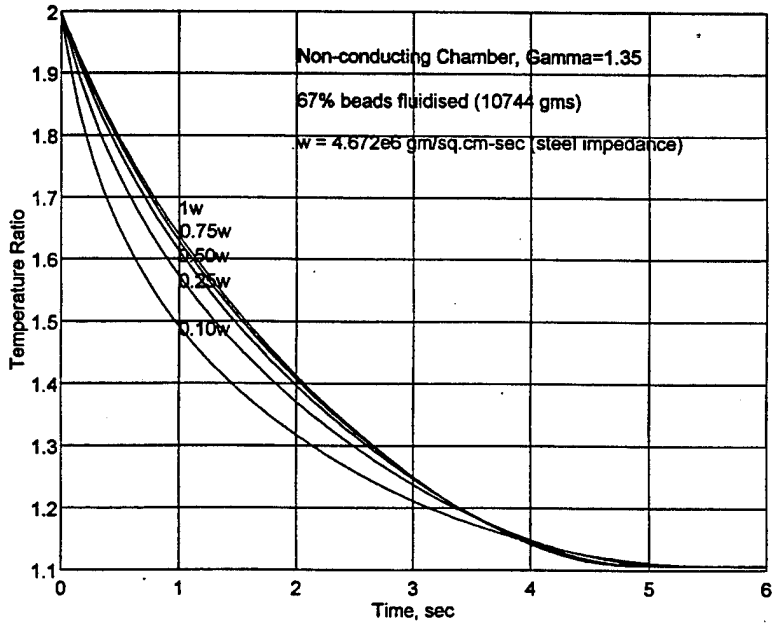

d.) Temperature ratio history.

Figure 4-5. Blast venting — effect of wall compliance (Continued).

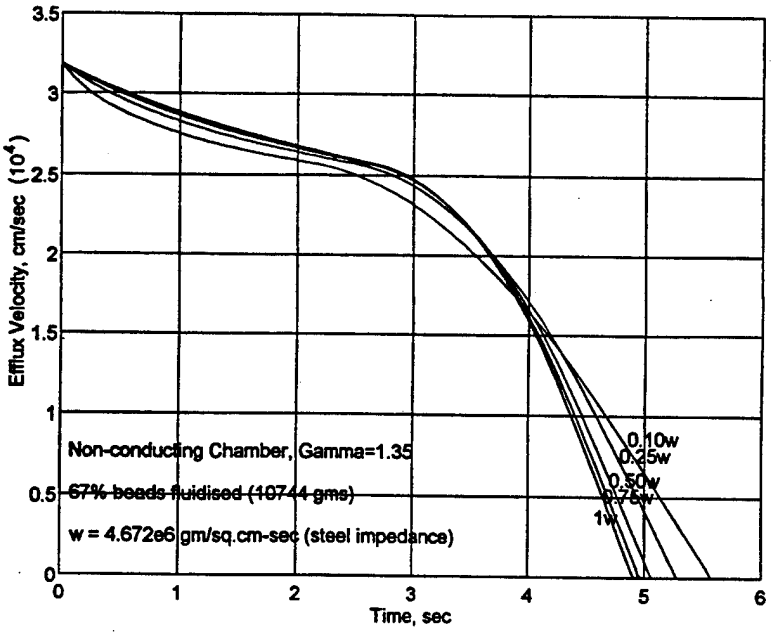

e.) Efflux velocity history.

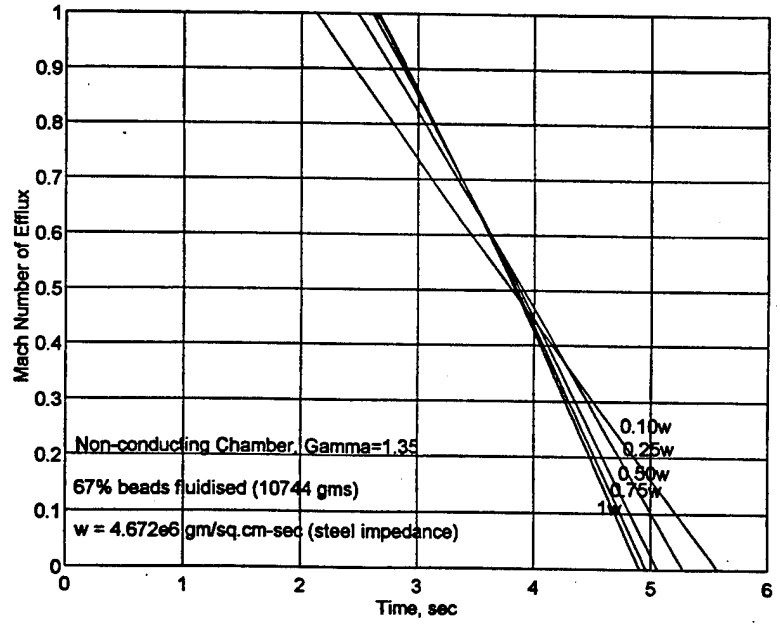

f.) Mach number history.

Figure 4-5. Blast venting — effect of wall compliance (Continued).

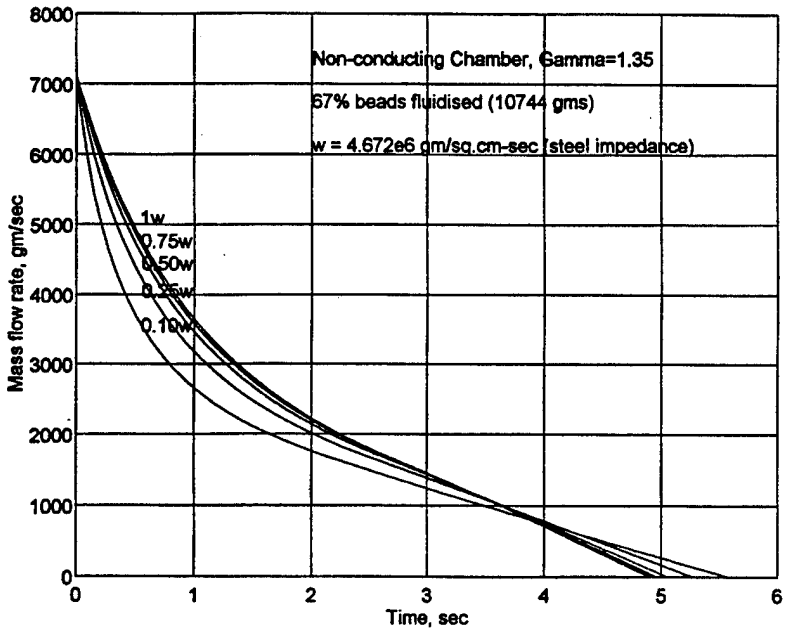

g.) Mass flow rate history.

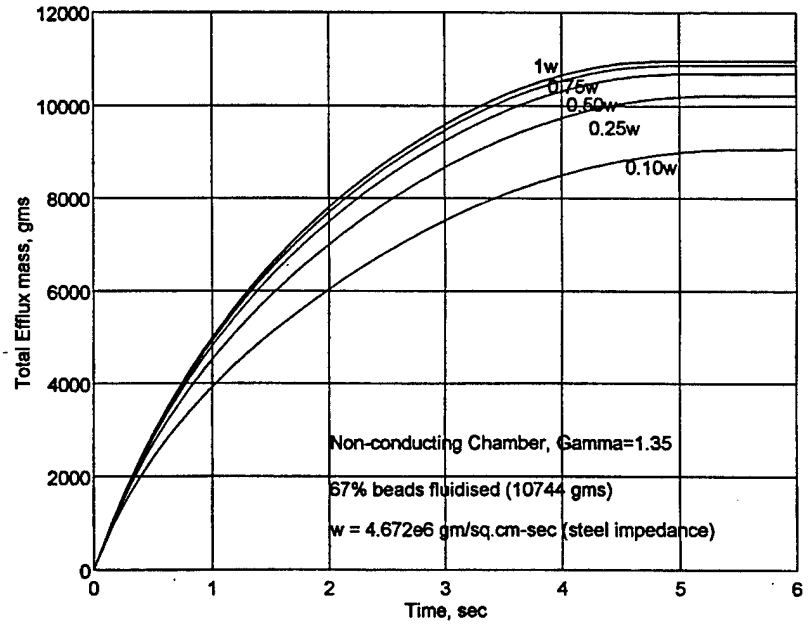

h.) Total efflux mass history.

Figure 4-5. Blast venting — effect of wall compliance (Continued).

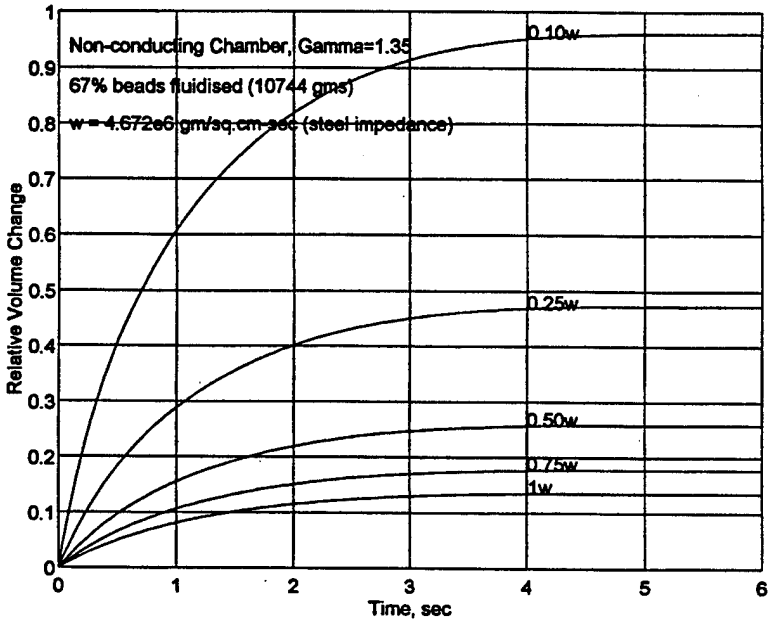

i.) Relative volume change history.

Figure 4-5. Blast venting — effect of wall compliance (Continued).

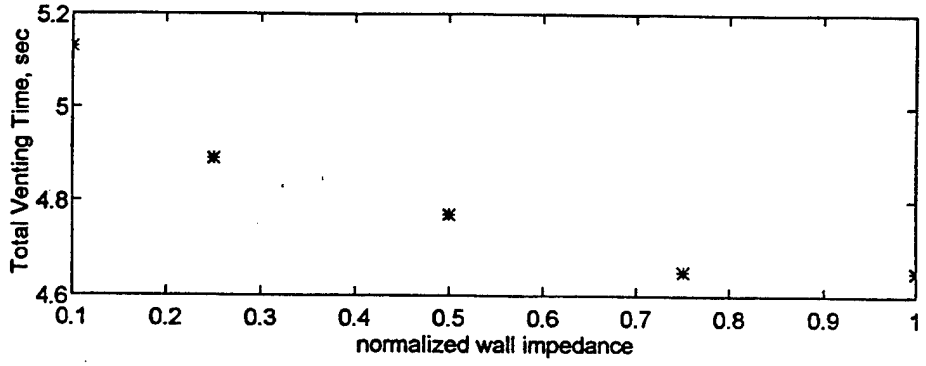

a.) Total venting time.

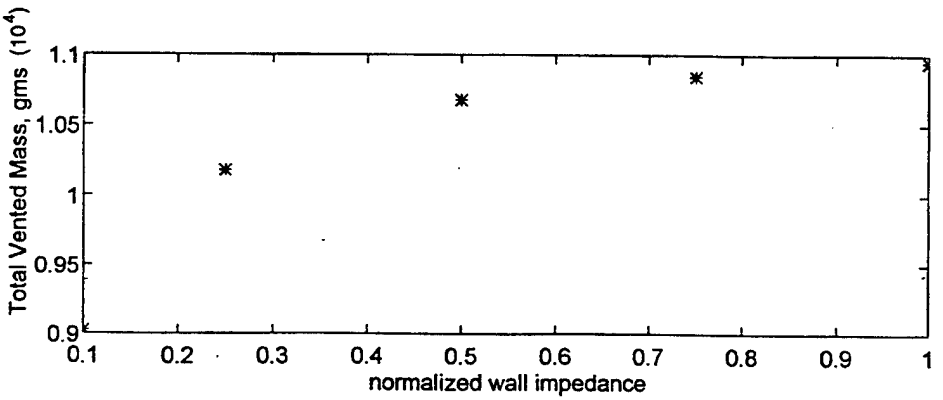

b.) Total vented mass.

Figure 4-6. Dependence of vent duration and vented mass on wall compliance.

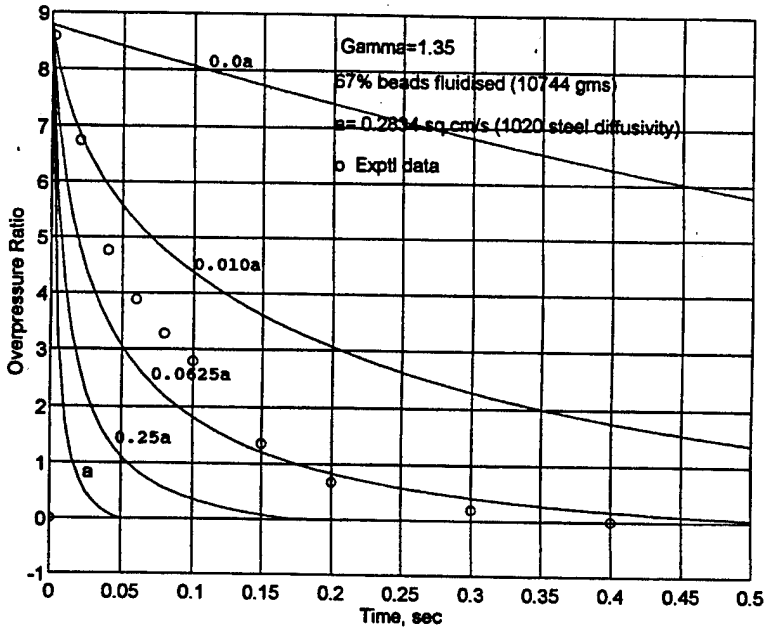

a.) Overpressure ratio history.

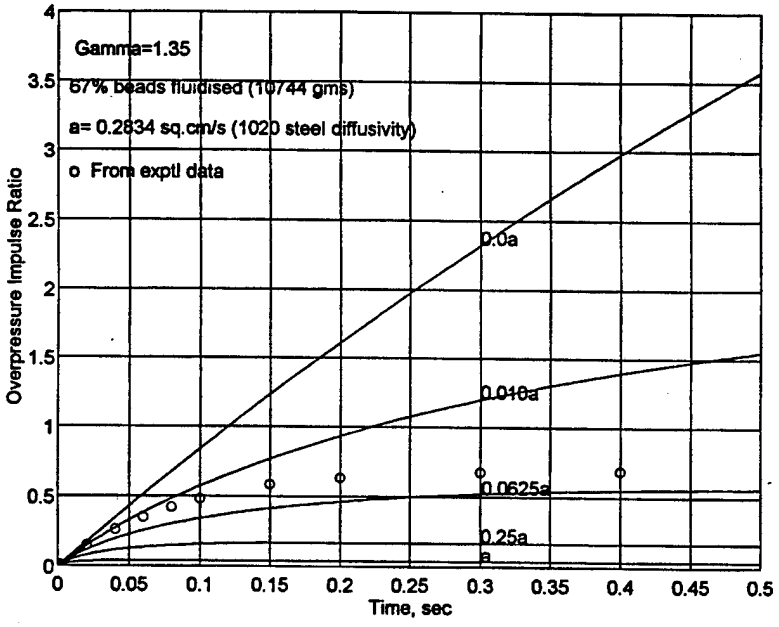

b.) Overpressure impulse ratio history.

Figure 4-7. Blast venting — heat loss by conduction only.

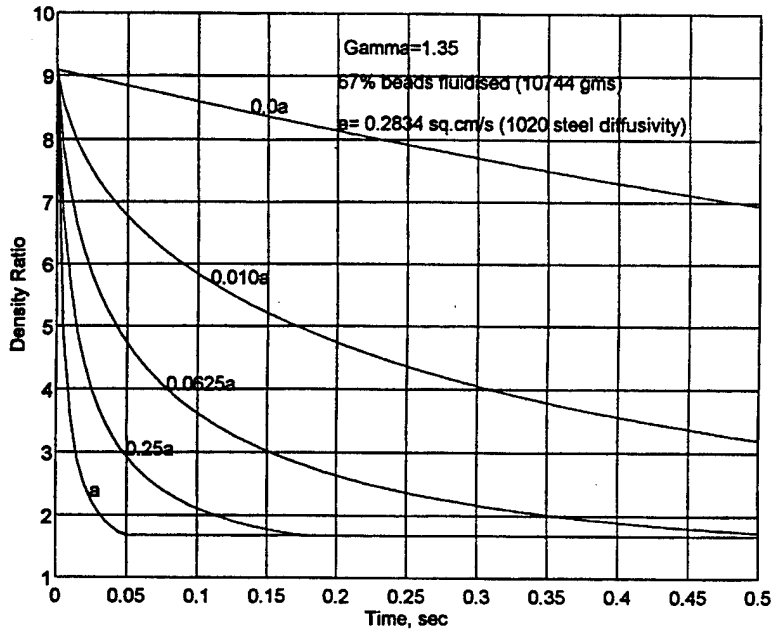

c.) Density ratio history.

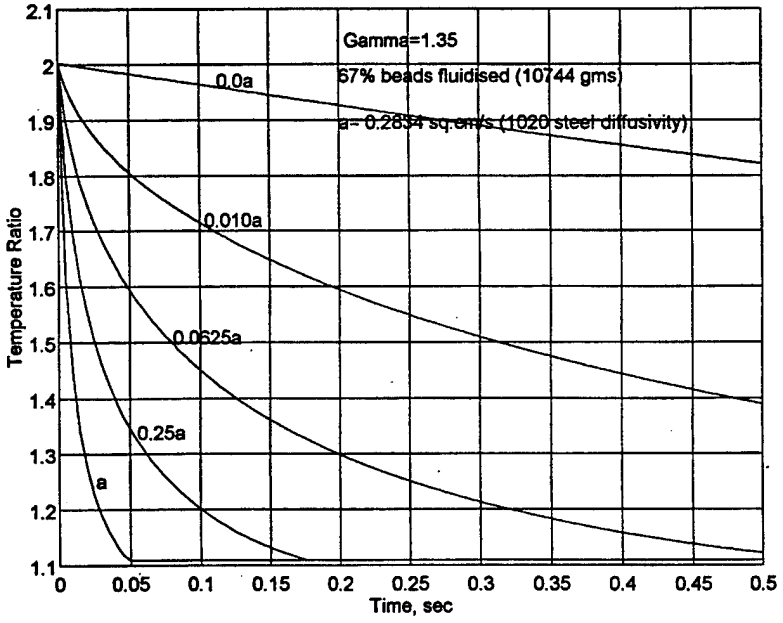

d.) Temperature ratio history.

Figure 4-7. Blast venting — heat loss by conduction only (Continued).

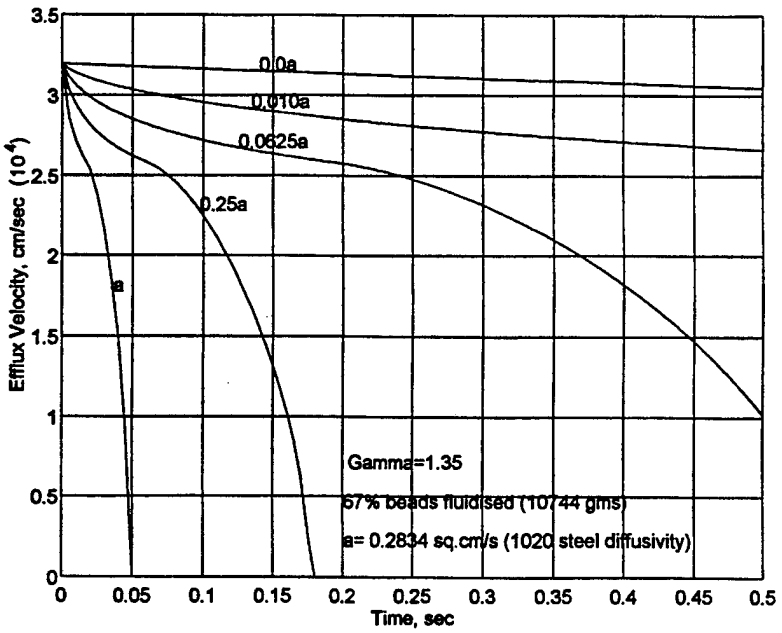

e.) Efflux velocity history.

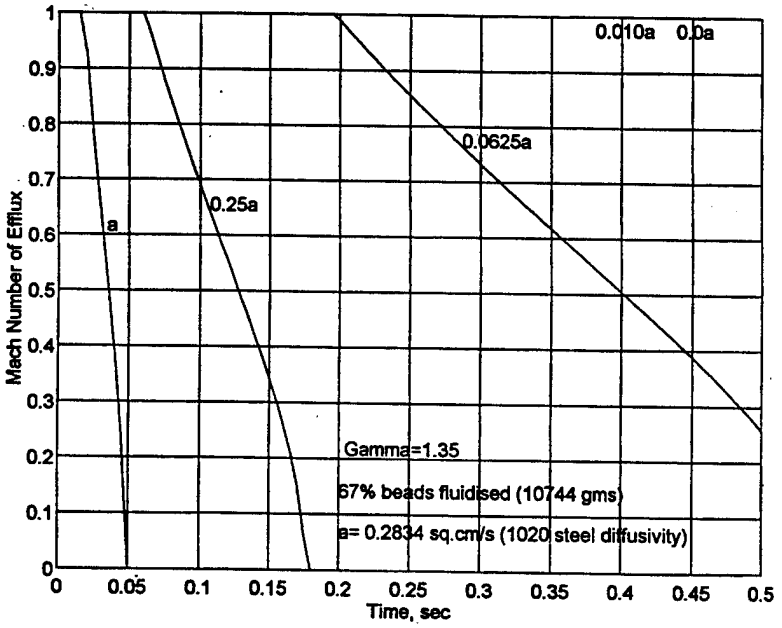

f.) Mach number history.

Figure 4-7. Blast venting — heat loss by conduction only (Continued).

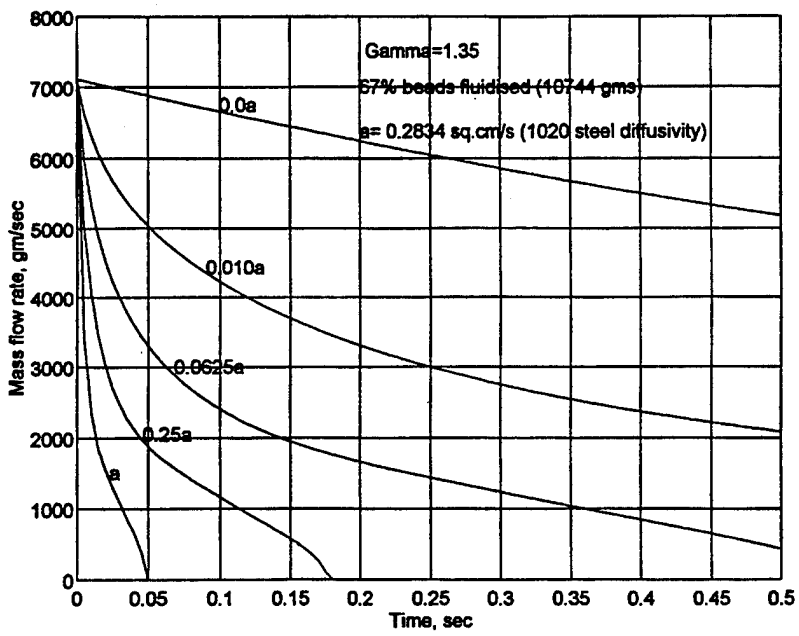

g.) Mass flow rate history.

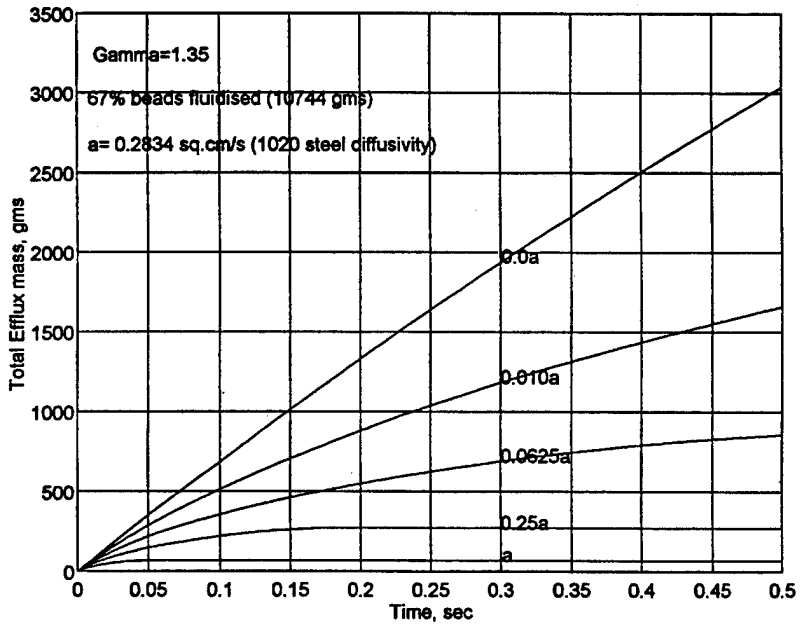

h.) Total efflux mass history.

Figure 4-7. Blast venting — heat loss by conduction only (Continued).

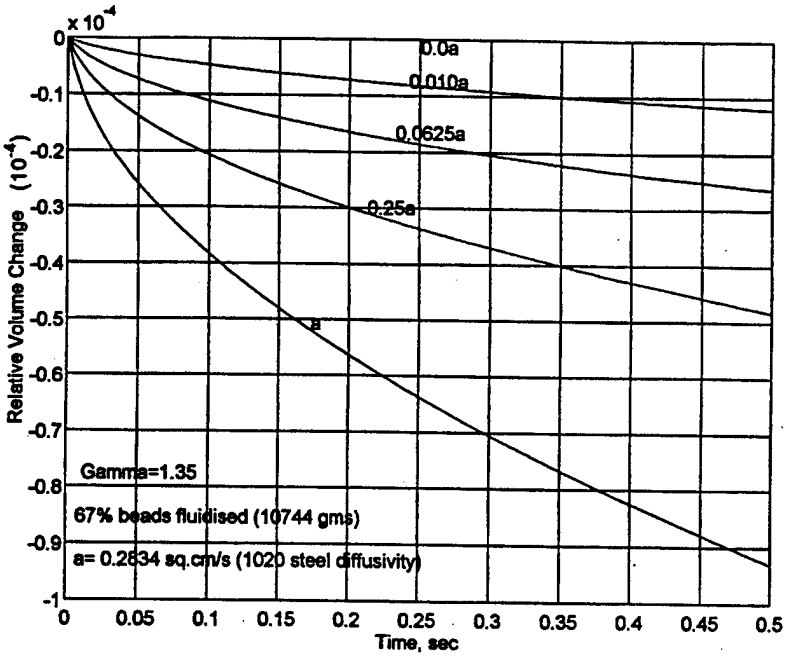

i.) Relative volume change history.

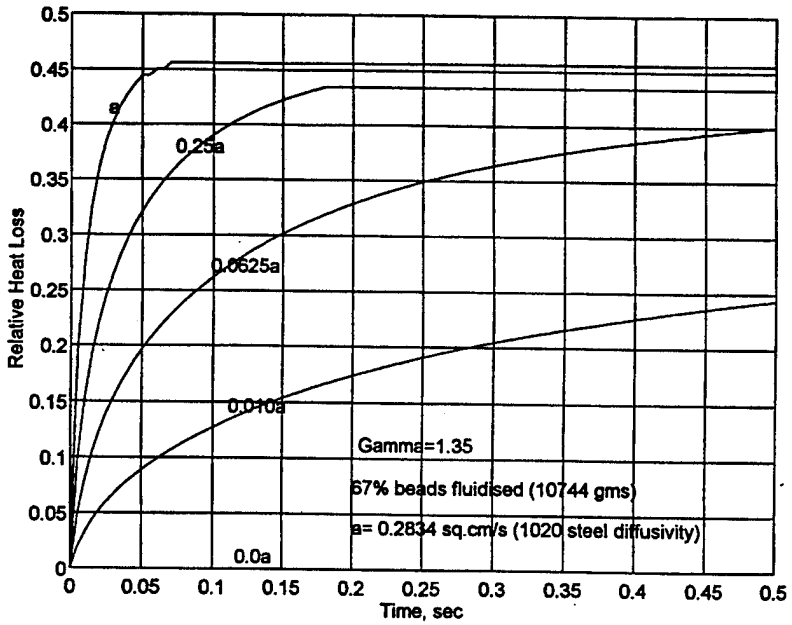

j.) Relative heat loss history.

Figure 4-7. Blast venting — heat loss by conduction only (Continued).

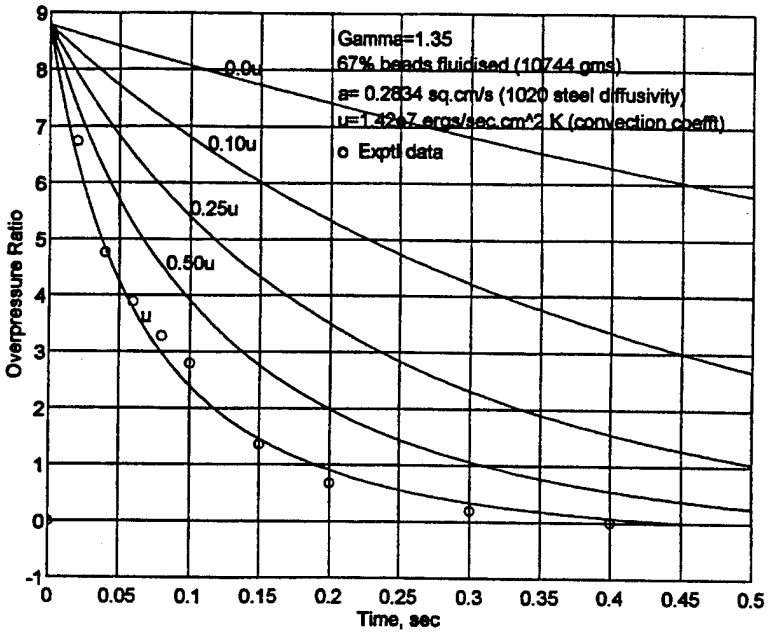

a.) Overpressure ratio history.

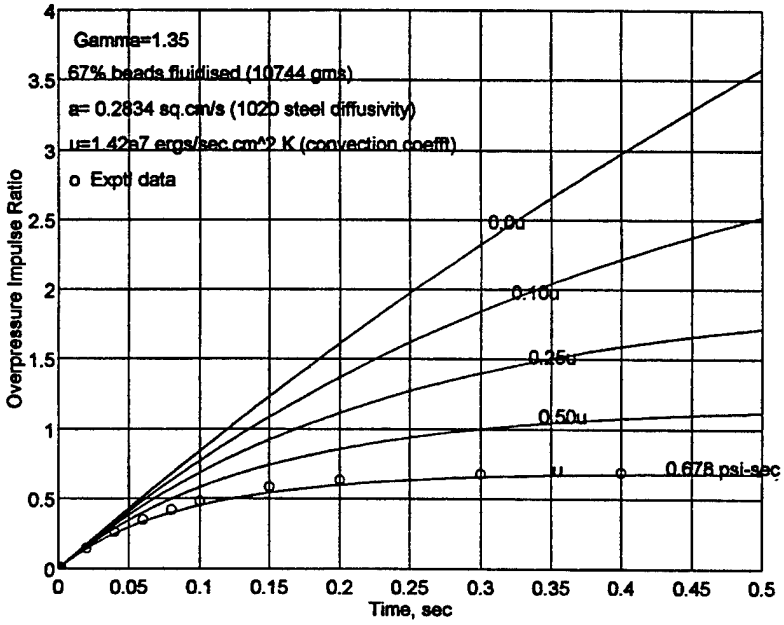

b.) Overpressure impulse ratio history.

Figure 4-8. Blast venting — heat loss by convection and conduction.

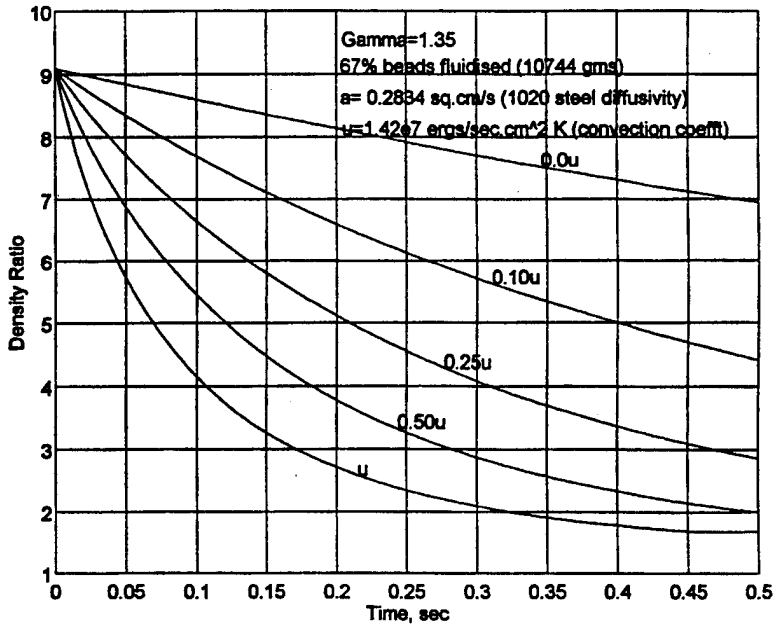

c.) Density ratio history.

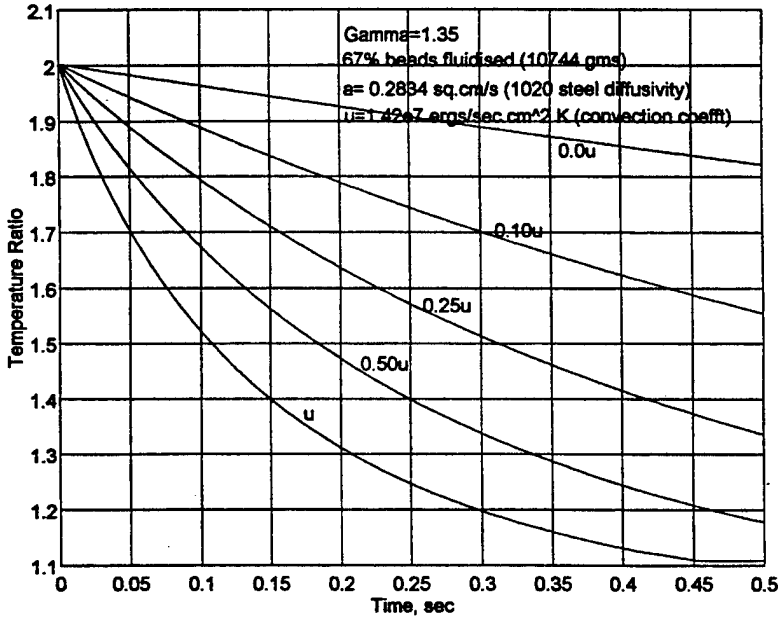

d.) Temperature ratio history.

Figure 4-8. Blast venting — heat loss by convection and conduction (Continued).

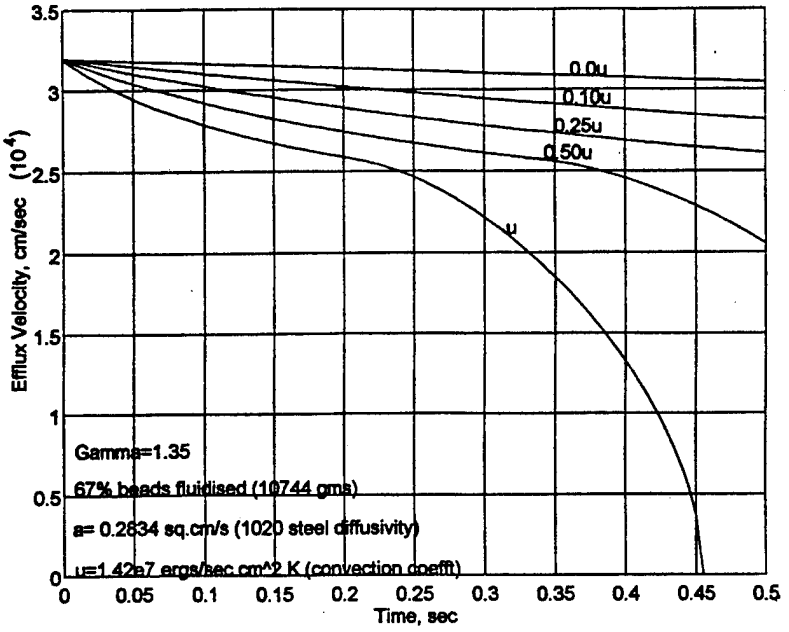

e.) Efflux velocity history.

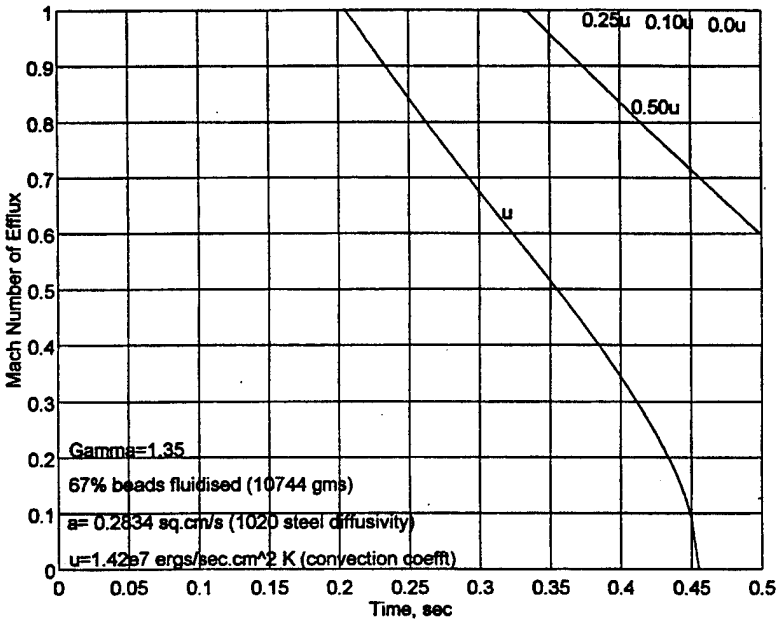

f.) Mach number history.

Figure 4-8. Blast venting — heat loss by convection and conduction (Continued).

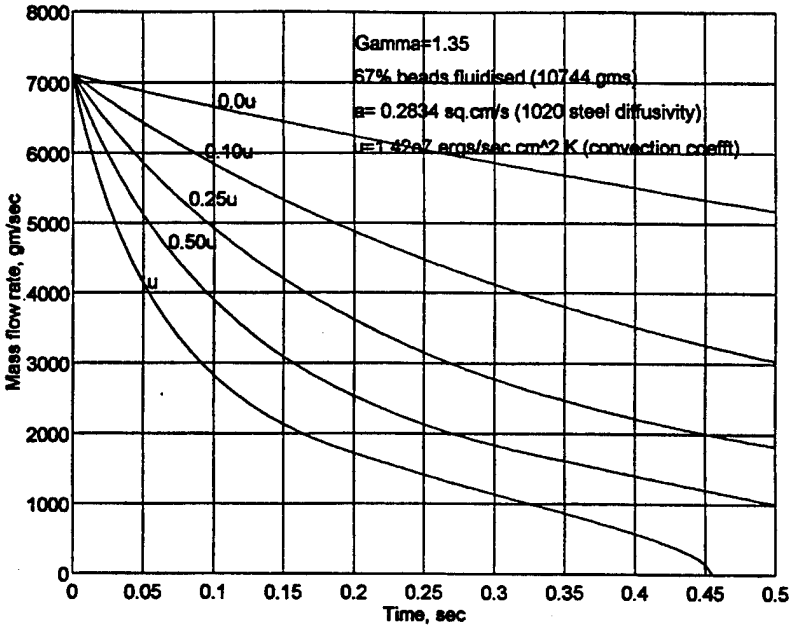

g.) Mass flow rate history.

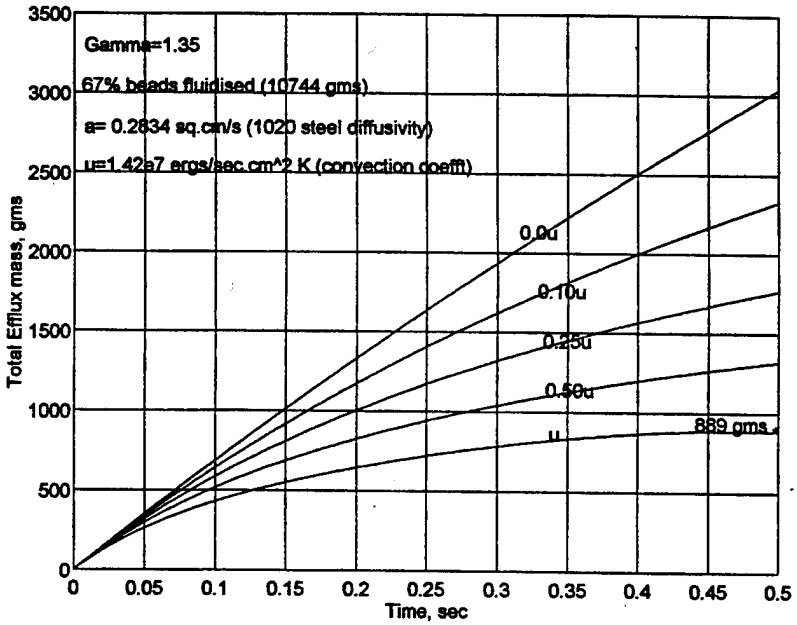

h.) Total efflux mass history.

Figure 4-8. Blast venting — heat loss by convection and conduction (Continued).

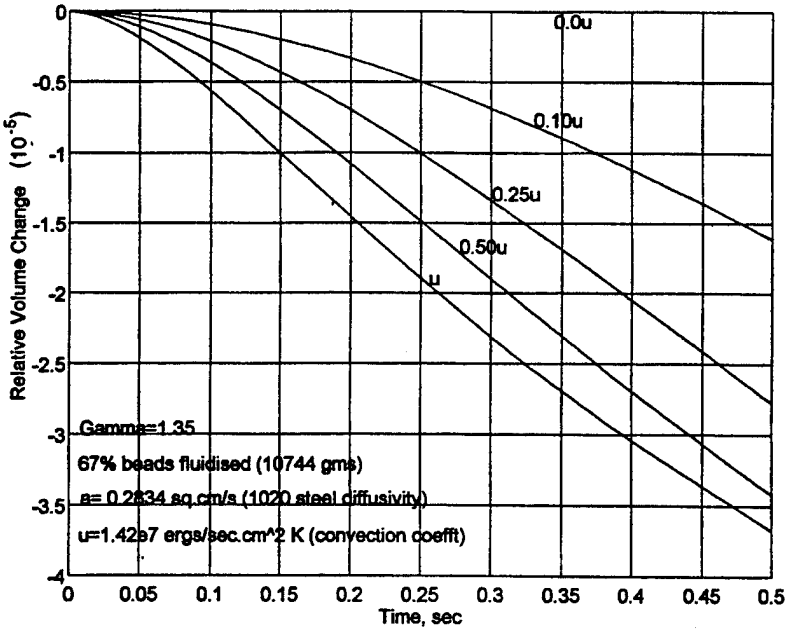

i.) Relative volume change history.

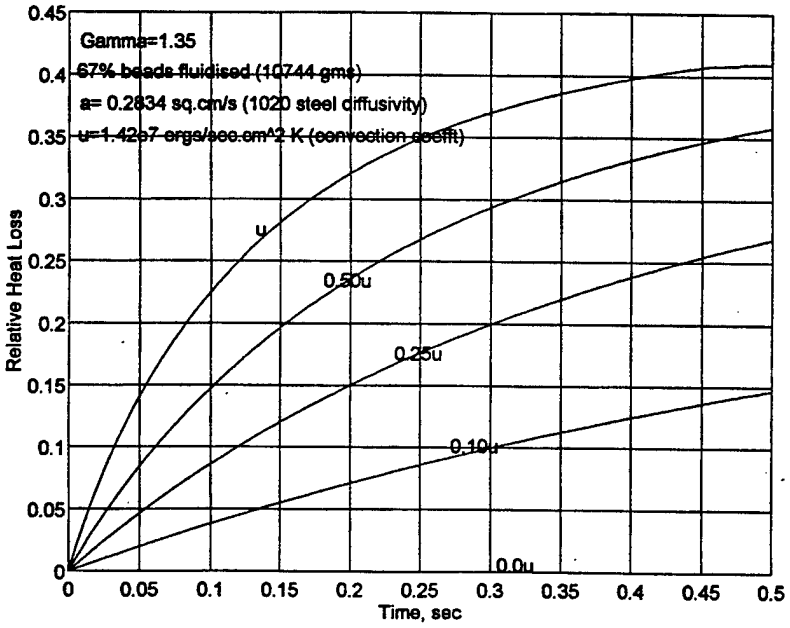

j.) Relative heat loss history.

Figure 4-8. Blast venting — heat loss by convection and conduction (Continued).

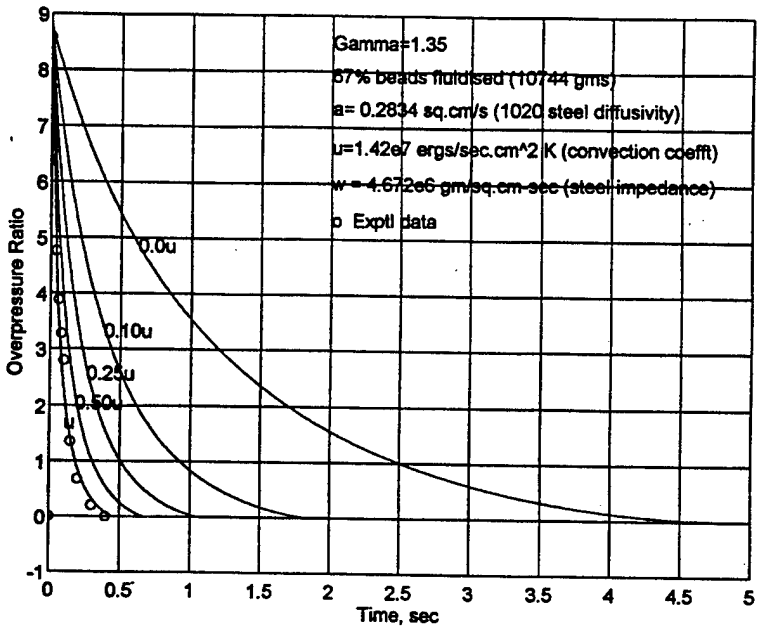

a.) Overpressure ratio history.

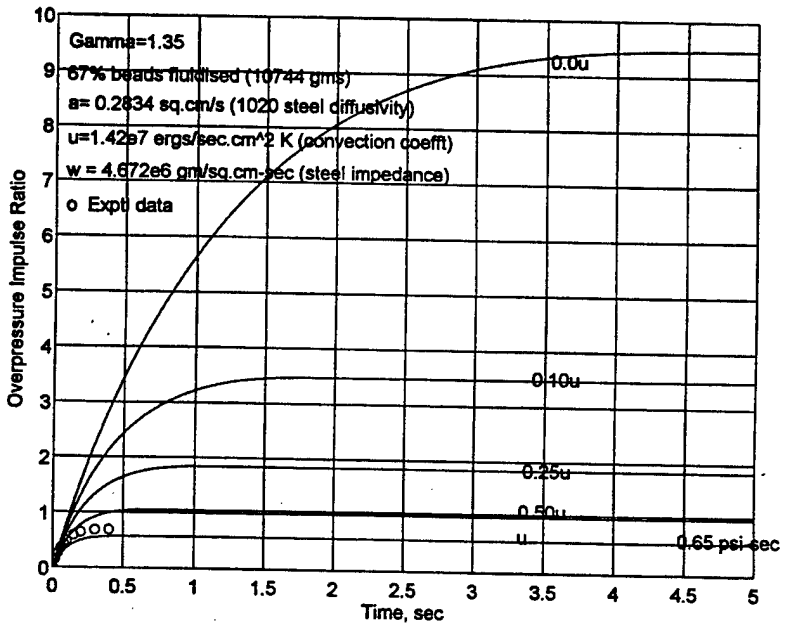

b.) Overpressure impulse ratio history.

Figure 4-9. Blast venting — fully responding.

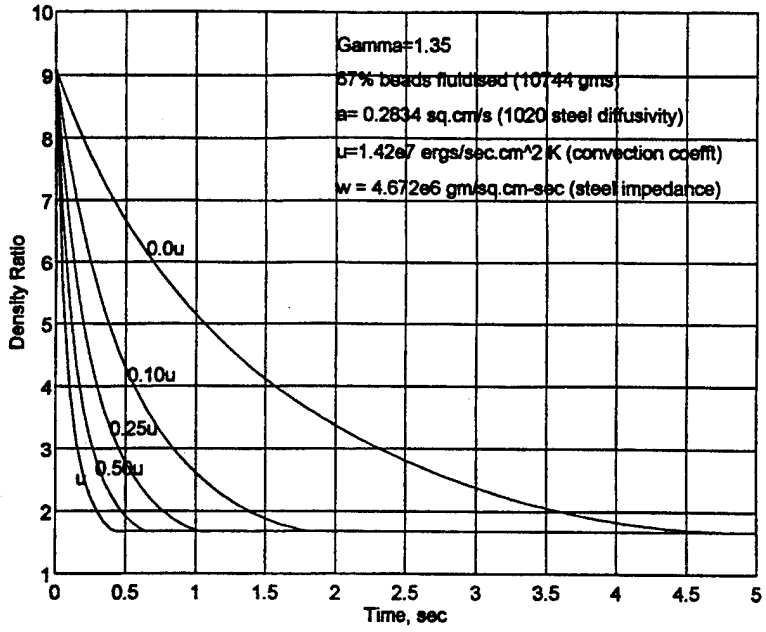

c.) Density ratio history.

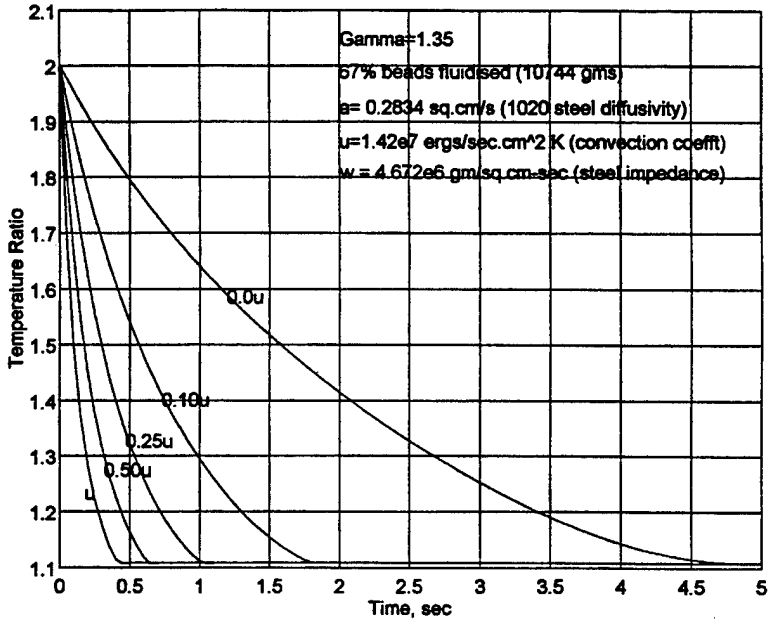

d.) Temperature ratio history.

Figure 4-9. Blast venting — fully responding (Continued).

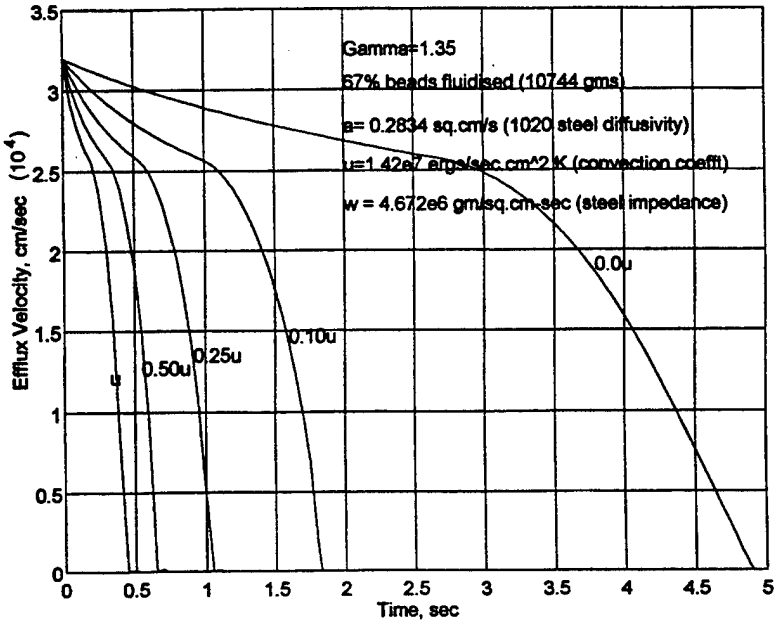

e.) Efflux velocity history.

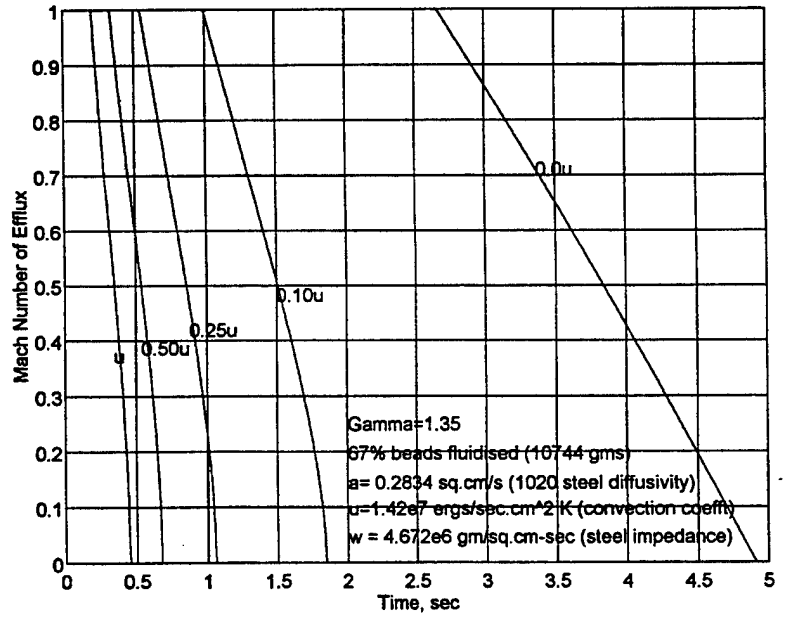

f.) Mach number history.

Figure 4-9. Blast venting — fully responding (Continued).

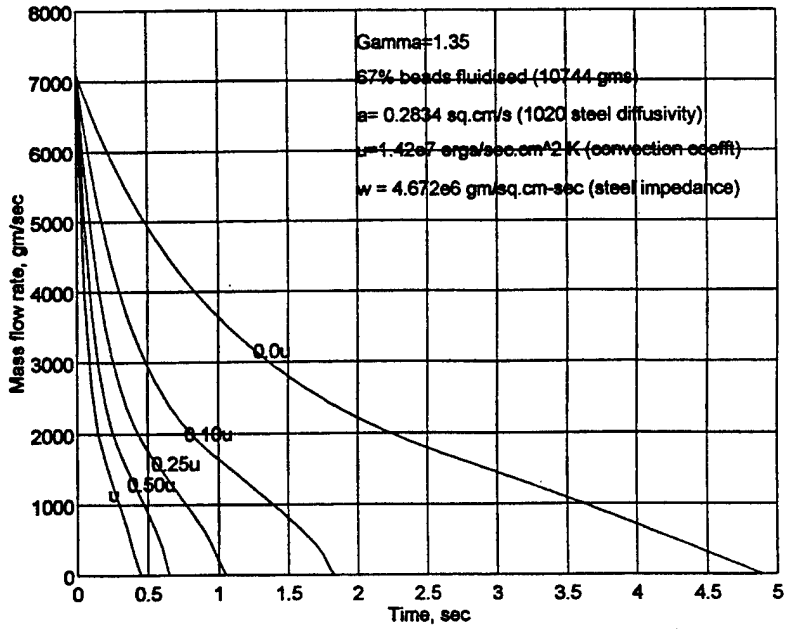

g.) Mass flow rate history.

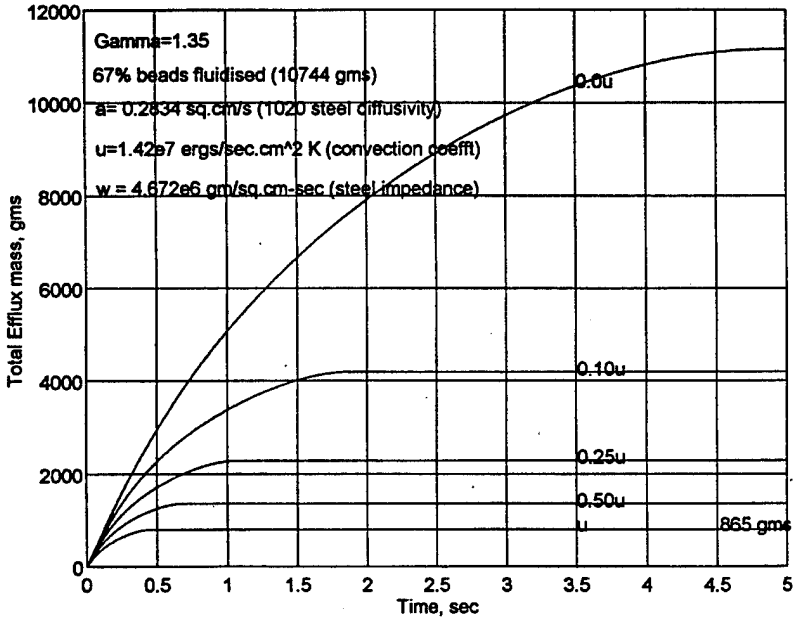

h.) Total efflux mass history.

Figure 4-9. Blast venting — fully responding (Continued).

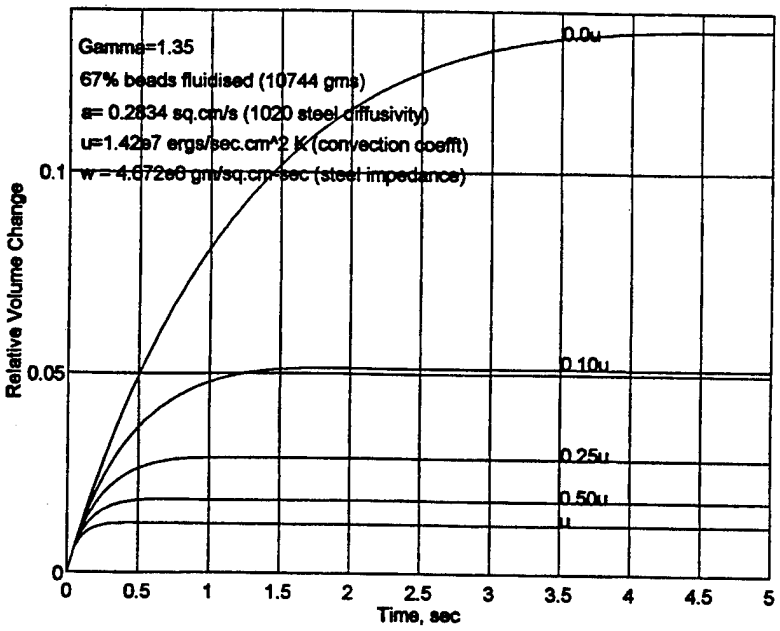

i.) Relative volume change history.

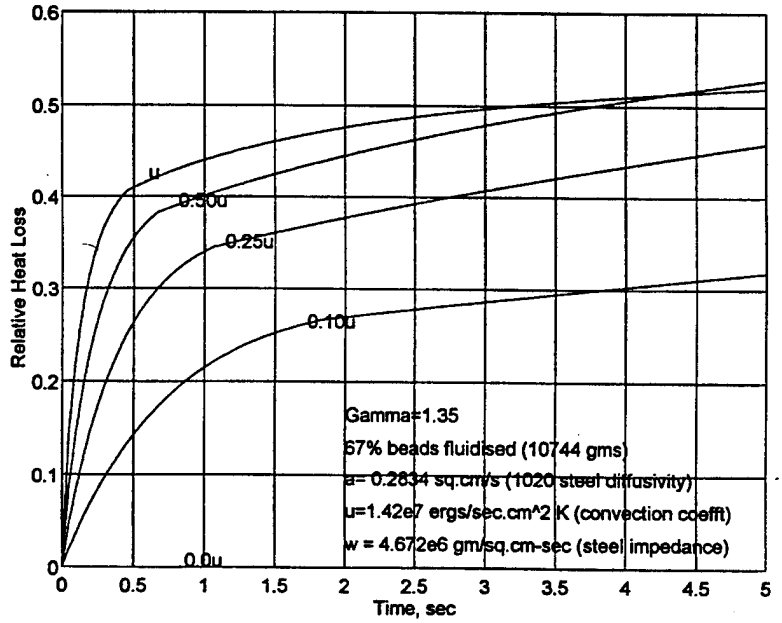

j.) Relative heat loss history.

Figure 4-9. Blast venting — fully responding (Continued).

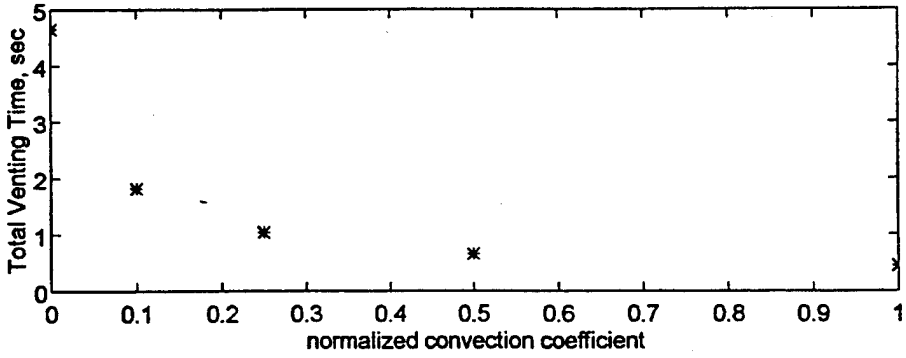

a.) Total venting time.

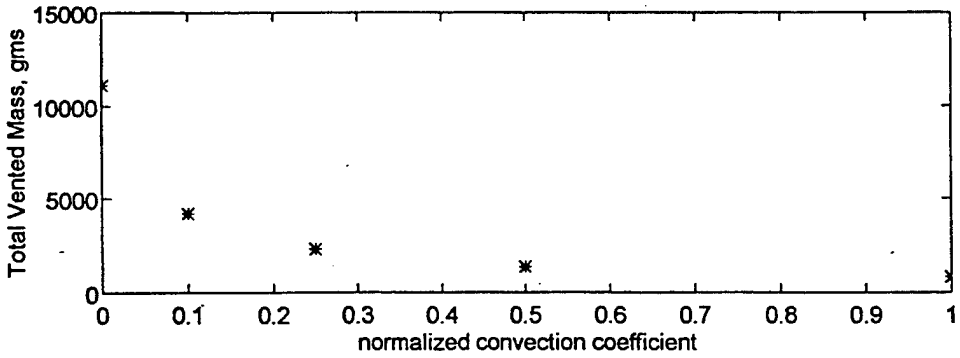

b.) Total vented mass.

Figure 4-10. Dependence of vent duration and vented mass on convection coefficient.

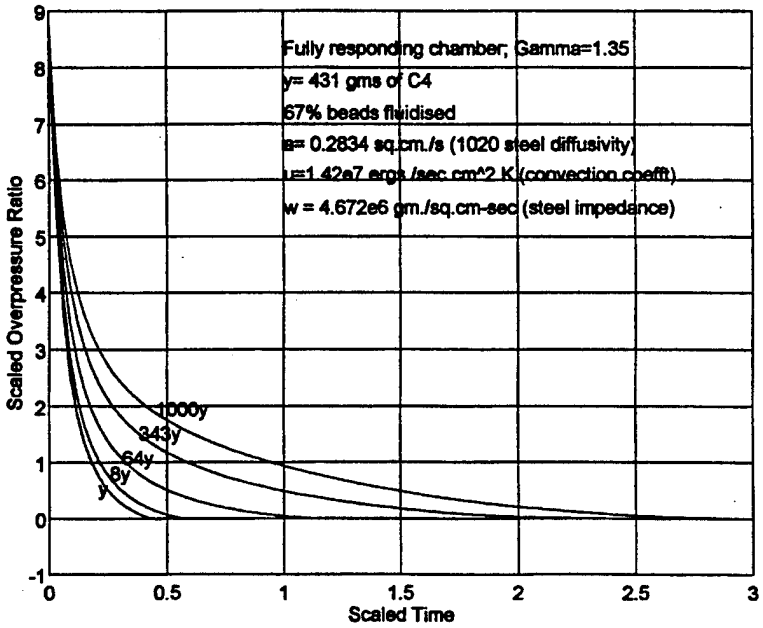

a.) Overpressure ratio history.

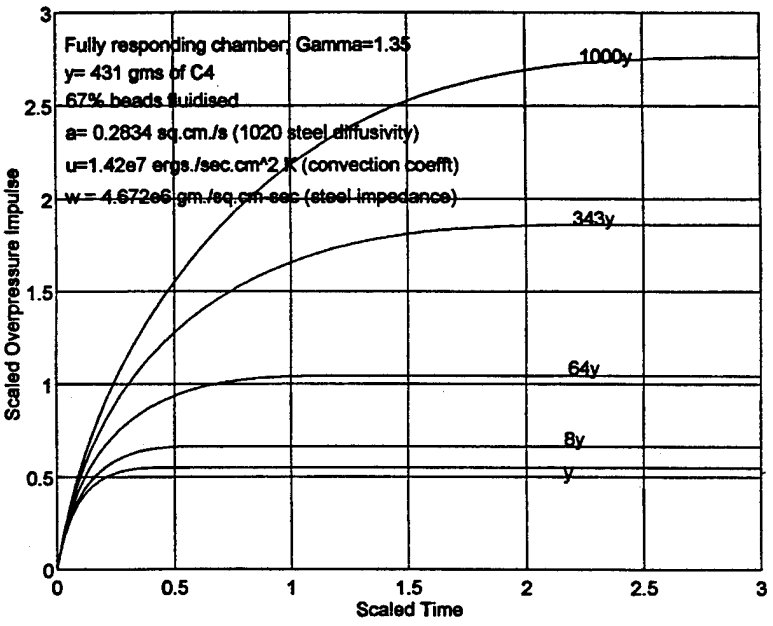

b.) Overpressure impulse ratio.

Figure 4-11. Scaled yield effects on venting — fully responding.

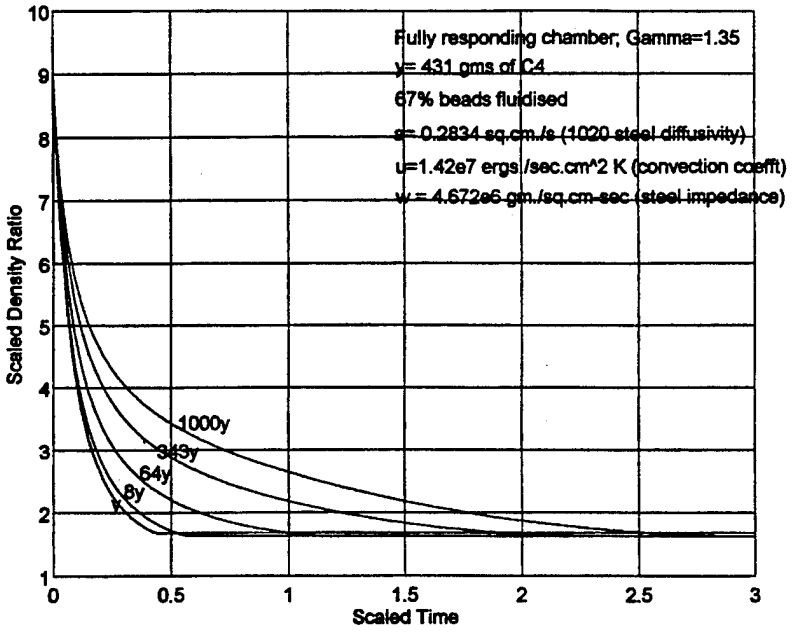

c.) Density ratio history.

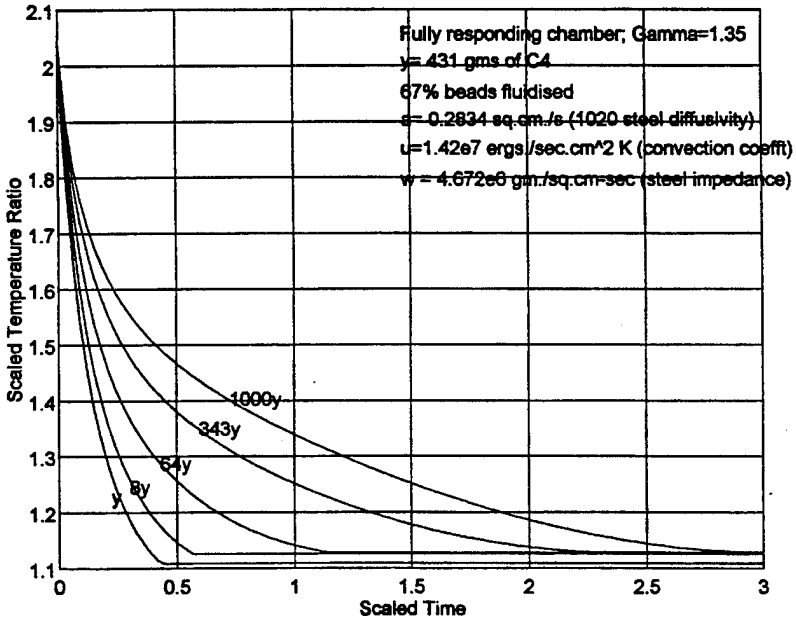

d.) Temperature ratio history.

Figure 4-11. Scaled yield effects on venting — fully responding (Continued).

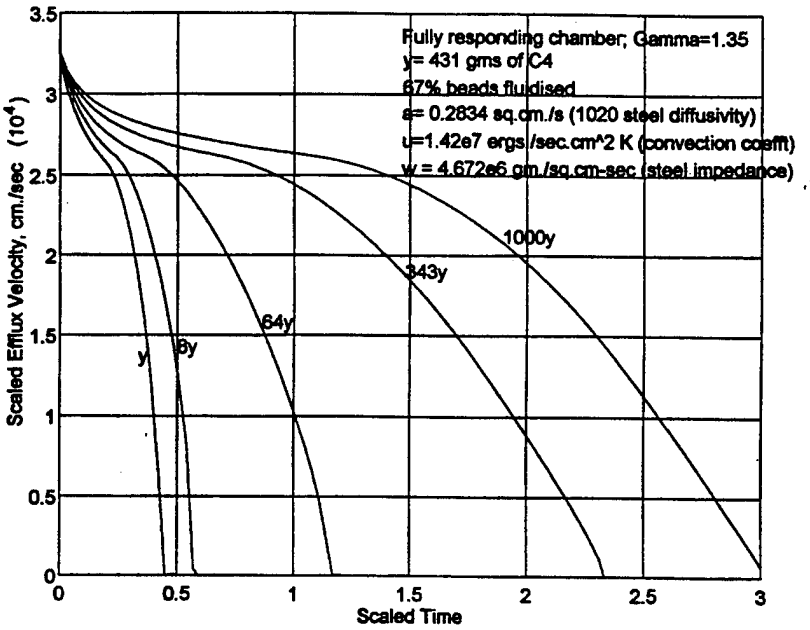

e.) Efflux velocity history.

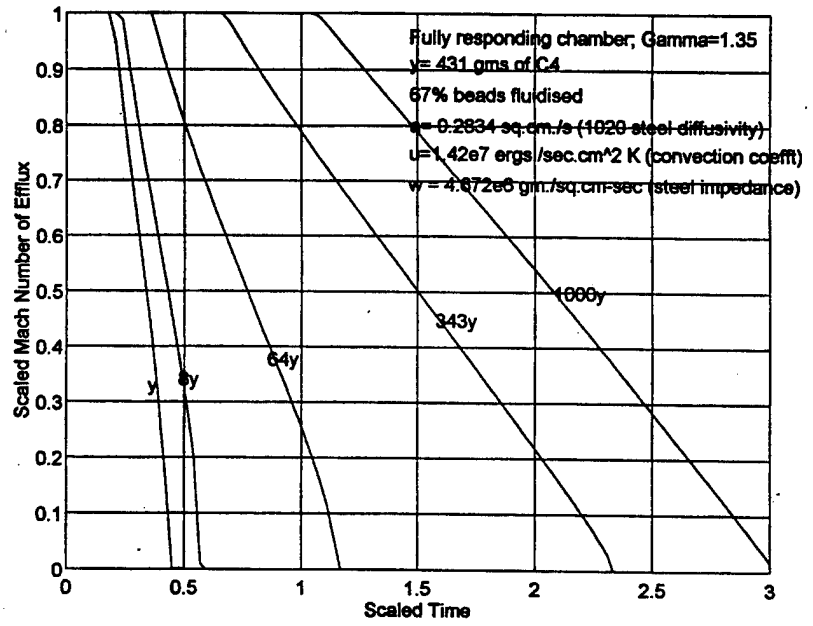

f.) Mach number history.

Figure 4-11. Scaled yield effects on venting — fully responding (Continued).

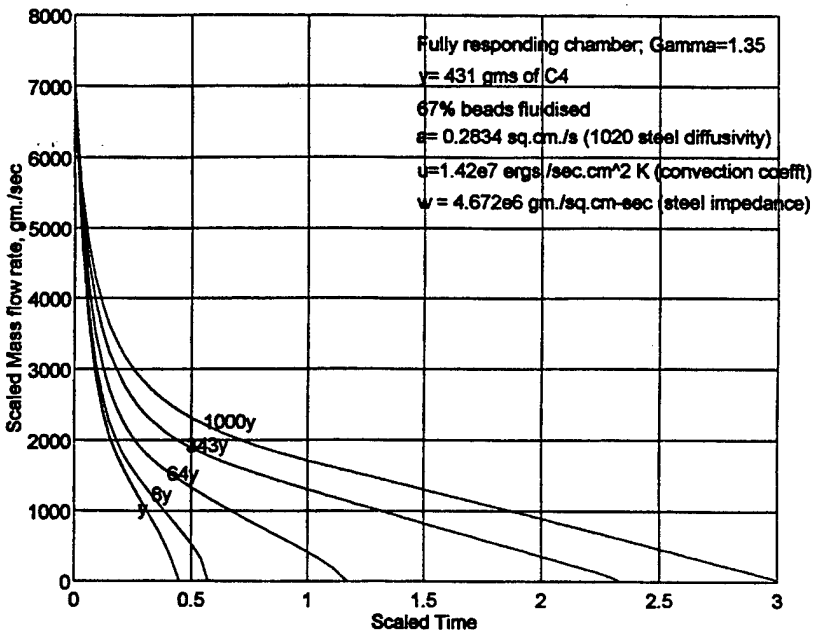

g.) Mass flow rate history.

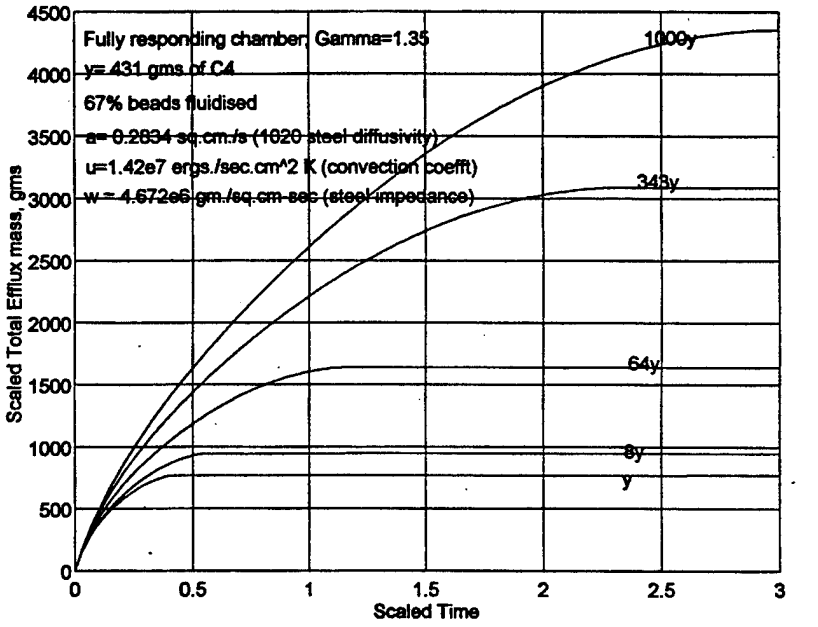

h.) Total efflux mass history.

Figure 4-11. Scaled yield effects on venting — fully responding (Continued).

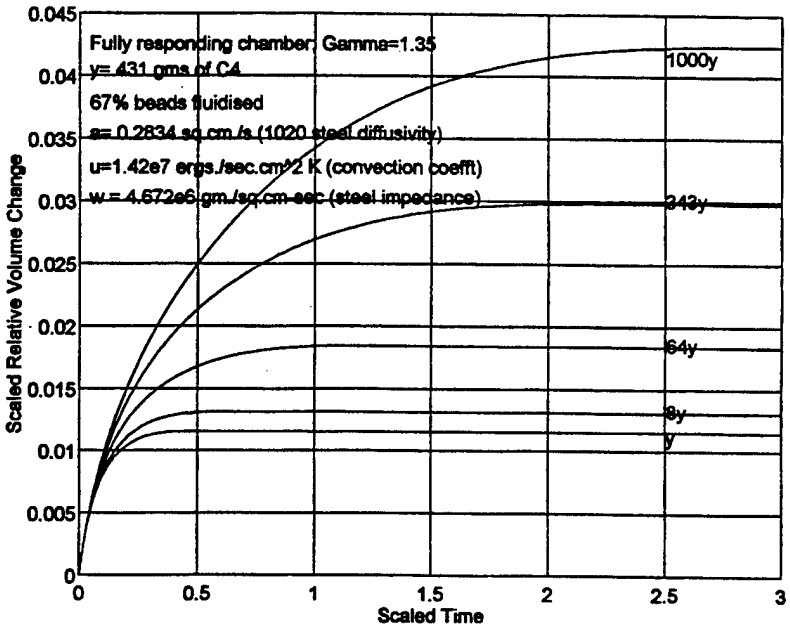

i.) Relative volume change history.

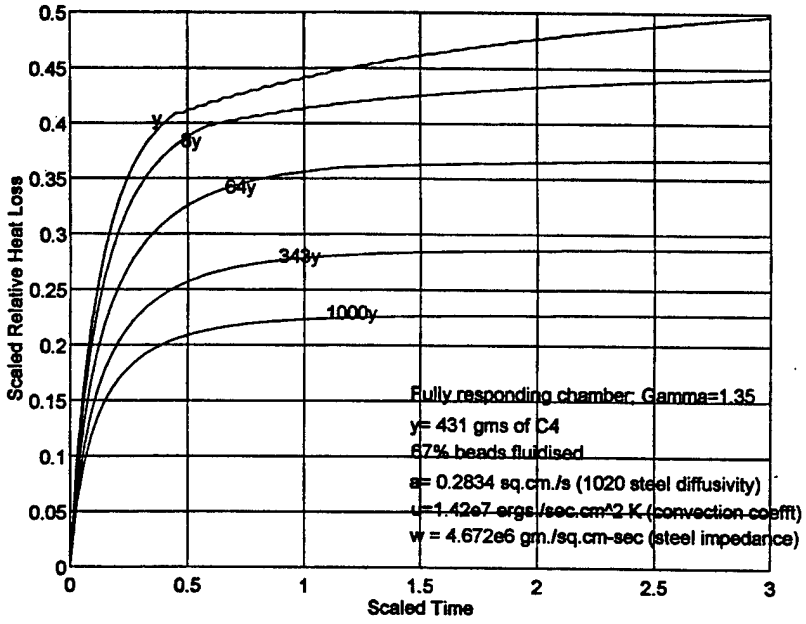

j.) Relative heat loss history.

Figure 4-11. Scaled yield effects on venting — fully responding (Continued).

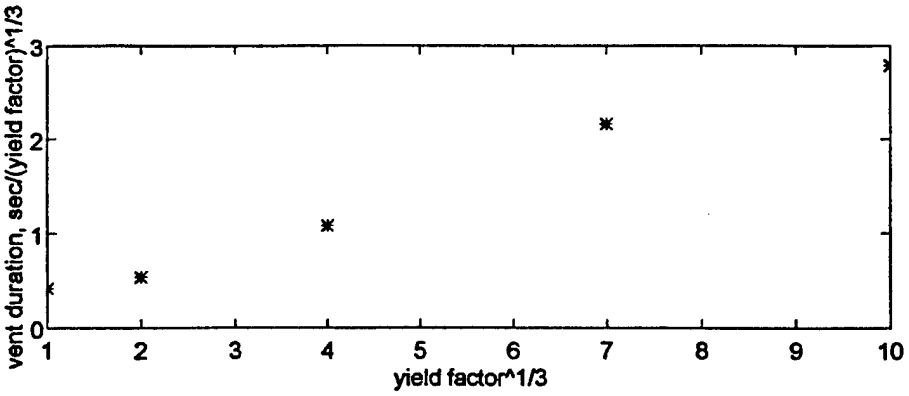

a.) Venting duration.

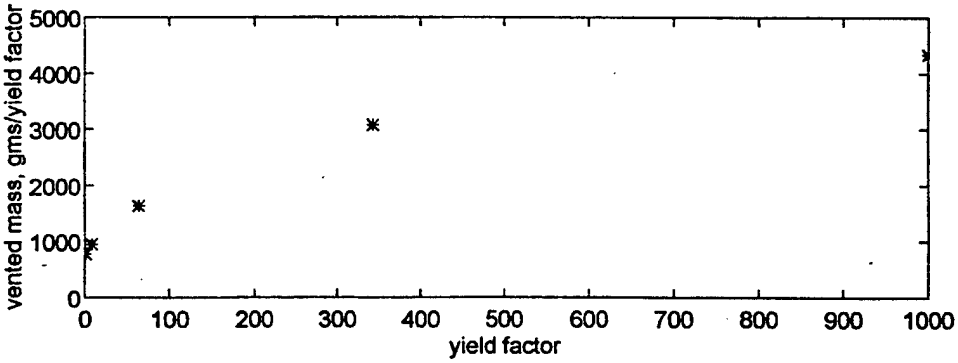

b.) Vented mass.

Figure 4-12. "Yield-scaled" vent duration and vented mass vs. scale factor for yield.

SECTION 5
DISCUSSION

The primary results obtained in the parametric studies of Section 4 are summarized in Table 5-1. Venting is most significantly affected by two factors, namely the fluidized fraction and the convection coefficient. Variations in γ and the wall impedance appear to be less important than the properties related to thermal effects, such as the convection coefficient and the diffusivity, in their effect on venting durations and vented masses. Conversion of the results of small scale experiments to large scale by simple yield-scaling becomes more complicated because of the non-scaling energy losses due to thermal effects. In particular, any predictions for venting durations and total vented masses for a large event based on yield-scaling of a small event are likely to be underpredictions, as shown by Figure 4-12.

The convection coefficient u is a quantity which depends in general on the geometry of the chambers, the physical and thermal properties of both chamber gases and chamber walls, the conditions of the wall surfaces, and the fluid mechanical regime in the chamber. It is not a well-established quantity for chamber explosions, although considerable effort has gone into its determination in other practical engineering applications (Reference 8). In forced convection problems, u is related to the Nusselt number. The range of values for convection coefficients is also quite large, going from 0.0003 J/sec $\cdot$ cm^2 $\cdot$ °K for heating (or cooling) of air to 28.4 J/sec $\cdot$ cm^2 $\cdot$ °K for dropwise condensation of steam (Reference 9). A value of 9.23 J/sec $\cdot$ cm^2 $\cdot$ °K has been suggested for the flow of liquid metals in pipes (Reference 2). The value 1.42 J/sec $\cdot$ cm^2 $\cdot$ °K appears to give MATVENT results in agreement with data from "Explusion Experiment No. 1" for a presumed fluidization fraction of 2/3. At present no experimental data are available to substantiate independently the selection of such a value. Other values (lower) of fluidization fraction and convection coefficient may also give results in agreement with experimental data. The convection coefficient depends on the mass flow rate in forced flow problems. Therefore, it is very likely that the convection coefficient for blast in responding chambers is dependent on the density and fluidized fraction of the hazardous material. For very small amounts of fluidized material, when the density of chamber gases approach the density of air, it is likely that the convection coefficient is two orders of magnitude smaller. There is a need for searching the literature and developing a formulation for the convection coefficient for problems of explosions in venting chambers.

The loose solid material in the chamber has been addressed in this report within the simple "dense -gas" approximation framework, wherein the solid material, explosion gases and chamber air behave as if the mixture constituted a single dense gas, with no drag or heat transfer between the particle and gas phases. The next level of analytical sophistication would be to employ the theory of interacting continua, where the solid and gaseous phases are treated as co-existing continua occupying the same volume, but capable of exchanging momentum by means of drag forces and energy by means of heat transfer. In reality, however, the particles are discrete, and particle-particle collision processes also will have to be taken into account, especially when the mass of the solid particles becomes large, in the exchange of momentum and energy. If inelastic particle collisions are included, energy losses due to plastic deformations have to be taken into account. Further complications are presented by the possibility of particle agglomerations, breakups, and subsequent size redistributions, all within a highly turbulent confined flow produced by an explosion. Phase changes from solid to liquid to gas can occur in regions where the temperatures are high enough and durations long enough, while condensation and solidification might occur in cooler regions. Estimations of heat transfer even to a single spherical particle of known thermal conductivity, density and specific heat capacity can be difficult because of uncertainties associated with surface characteristics (represented in the convection coefficient). For example, in the absence of any surface resistace to heat transfer, a glass sphere of 0.01 cm diameter (κ =0.85 J/sec· cm ·°K and a = 0.0046 cm^2/sec, approximately, for common glass) attains temperature equilibrium with a surrounding hot air medium in approximately 5 msec; however the same sphere will not heat up at all if the surface were to be insulated. These uncertainties are not addressed by the simple model presented.

The MATVENT model has also not considered the following factors: (a) loss of energy due to heating and vaporization of the hazardous material, (b) heat addition to the chamber gases due to any exothermic reactions in the material being vaporized, (c) heat additions due to condensation of hazardous material vapors near the (cooler) wall surfaces, (d) the effect of increased wall area accompying changes in the chamber volume, (e) the effect of any changes in the vent area during venting, and (f) the effect produced by constriction of the jet of venting gases at the orifice.

For high-yield explosions (a), (b) and (c) are probably minor effects. In the case of (d), a separate calculation (not reported here) for fully responding chambers in which the wall area was allowed to change proportionally as the two-thirds power of the chamber volume, failed to show any significant differences from the "fully responding" case (Section 4.3.6).

Table 5-1. Summary of parameter variation effects on venting.

Quantity	increasing γ	increasing f	increasing w	increasing a	increasing u
Overpressure	increases	increases	initially same,then increases	decreases	decreases
Overpr Impulse	increases	increases	increases	decreases	decreases
Density	decreases	increases	initially same,then increases	decreases	decreases
Temperature	increase then decrease	decreases	initially same,then increases	decreases	decreases
Efflux Velocity	increases	increase then decrease	initially same,then increase/ decrease	decreases	decreases
Choking Duration	increases	increases	increases	decreases	decreases
Mass flow rate	increases	increases	increases	decreases	decreases
Total Efflux mass	increases	increases	increases	decreases	decreases
Volume change	-------	-------	decreases	decreases	decreases
Heat loss	-------	-------	-------	increases	increases
Venting duration	little effect	increases	decreases	decreases	decreases
Total Vented mass	increases	increases	increases	decreases	decreases

Vent area changes during efflux may be significant in estimating vented masses and venting durations; a reasonable model for such changes needs to be developed. Jet constriction effects, which depend upon vent pipe length and geometry, can be taken into account by means of an "orifice coefficient" such as that for a Borda tube. It is possible to incorporate all of the foregoing effects into future versions of MATVENT.

SECTION 6
CONCLUDING REMARKS

A simple PC-based code named MATVENT has been developed, described and employed to carry out parametric calculations on the effects of varying γ, varying the fluidization fraction, varying the chamber wall impedance, varying the chamber wall diffisivity and varying the convection coefficient in several separate studies. The response models provide an approximate, but convenient, method in assessing the relative importance of factors which affect venting. The approximate nature of the models is consistent with the current state of knowledge on venting from blast in chambers. The effects of chamber response on yield- scaling of venting durations and vented masses is also examined with MATVENT runs. It is shown that yield-scaling based on small scale experiments may lead to significant underpredictions of venting durations and vented masses in a large scale event. The parametric calculations show that attention must be paid to thermal response, and to a lesser extent, the mechanical response, of the chamber wall materials in designing small scale experiments on internal blast and venting. The chamber materials must be carefully chosen and the internal surfaces of the chamber must be carefully designed to achieve the purpose of the experiments.

MATVENT provides a tool for quick (a minute or so per calculation on a 486 PC platform) trade-off studies in experiment design. MATVENT can also be useful when conventional scaling rules become uncertain in the calculation of potential full scale scenarios.

Further, MATVENT can be extended to treat cases of venting from multiple interconnected chambers in one of which a blast might be set off. Further research needs exist in establishing a formulation for convection coefficients under chamber blast conditions, and in particular, the dependence of convection coefficients on the properties of chamber gases. Extensions to the current MATVENT model will be helpful in assessing the relative sensitivity of venting durations and vented masses to factors such as vent area changes during venting, jet constriction effects and vaporization, condensation as well as reaction characteristics of stored hazardous materials.

SECTION 7
REFERENCES

1. Owczarek, J.A., - " Fundamentals of Gas Dynamics"(U), International Textbook Company, 1955.(Unclassified)

2. Schneider, P.J., - " Conduction Heat Transfer"(U), Addison - Wesley Publishing Company, 1964.(Unclassified)

3. The MathWorks, Inc., - "MATLAB User's Guide For Microsoft Windows"(U), February 1993.(Unclassified)

4. Ganong, G.P. -"WES Test details"(U), Private Communication.(Unclassified)

5. Dobratz, B.M., and Crawford, P.C., - " LLNL Explosives Handbook"(U), UCRL - 52997 Change 2, January 31, 1985.(Unclassified)

6. " CRC Handbook of Chemistry and Physics"(U), 73rd edition, 1992-93.(Unclassified)

7. Ganong, G.P. - Private Communication.(Unclassified)

8. Adams, W.H., - " Heat Transmission"(U), - Third Edition, McGraw Hill Book Company, 1954.(Unclassified)

9. Bennett, C.O. and Myers, J.E., - " Momentum, Heat and Mass Transfer"(U), McGraw Hill Book Company, 1962.(Unclassified)

APPENDIX A

MODELING EQUATIONS

$$\mathrm{w} = \rho_{\mathrm{w}} \cdot c_{\mathrm{w}}$$

$$\xi = u/\left\{\rho_{\mathrm{w}} \cdot C \cdot \kappa\right\}^{0.5}$$

$$\rho_{0c} = \left\{\rho_{0a} V_0 + M_{ex}\right\}/V_0$$

$$R_0 = \rho_{0g}/\rho_{0a}$$

$$c_{0ag} = \left\{\gamma \cdot p_{0a}/\rho_{0g}\right\}^{0.5}$$

$$x_{0g} = \left[1 + \left\{(\gamma - 1) \cdot W/(V_0 \cdot p_{0a})\right\}\right]$$

$$p_0 = p_{0a} \cdot x_{0g}$$

$$x_{cg} = x_{0g}^{(1-\gamma)/\gamma}$$

$$c_{0g} = c_{0ag} \cdot \sqrt{x_{0g}}$$

$$c_{0cr} = c_{0g} \cdot \sqrt{2/(\gamma + 1)}$$

$$\Theta_0 = \left[1 + \gamma \cdot W/(C_p \cdot \rho_{0g} \cdot V_0 \cdot T_{0a})\right]$$

$$T_0 = T_{0a} \cdot \Theta_0$$

$$\Theta_{cg} = x_{cg} \cdot \Theta_0$$

$$x_g = p_g/p_{0a}$$

$$\Theta_g = T_g(t)/T_0$$

$$\beta_0 = \left\{(C/C_p) \cdot (\rho_w/\rho_{0g}) \cdot (AR_0/V_0) \cdot \sqrt{\mathrm{a}}\right\}$$

$$\Lambda = AR_0 \cdot p_{0a}/\mathrm{w}$$

$$B = AR_0 \cdot T_{0a} \cdot \epsilon \cdot \sqrt{\mathrm{a}}$$

$$\chi = \left\{(\gamma + 1)/2\right\}^{\gamma/(\gamma-1)}$$

$$\rho_{0cr} = \rho_{0g} \cdot \left[2/(\gamma + 1)\right]^{1/(\gamma-1)}$$

$$U_0 = c_{0cr}$$

$$\dot{m}_0 = a_0 \cdot \rho_{0cr} \cdot U_0$$

$$M_0 = 1$$

if $x_{0g} < \chi$,

$$\dot{m}_0 = a_0 \cdot \sqrt{(\gamma+1)/(\gamma-1)} \cdot \rho_{0g} \cdot c_{0cr} \cdot \left[x_{0g}^{-2/\gamma} - x_{0g}^{-(\gamma+1)/\gamma}\right]^{1/2}$$
$$U_0 = \dot{m}_0/(a_0 \cdot \rho_{0cr})$$
$$M_0 = \sqrt{2/(\gamma-1)} \cdot \left\{x_{0g}^{(\gamma-1)/\gamma} - 1\right\}^{1/2}$$

Fluid Mechanical Model-Quasi steady treament for the rate of change of pressure in the chamber:

$$x_g(t) = x(t)$$

if $\Theta_g(t) > \Theta_{cg}$,

$$\dot{x}_g(t) = -\gamma\left\{(\gamma+1)/2\right\}^{-(\gamma+1)/2(\gamma-1)} \cdot c_g(t) \cdot (A/V) \cdot x_g^{(3\gamma-1)/2\gamma}$$

if $\Theta_g(t) \leq \Theta_{cg}$,

$$\dot{x}_g = 0$$

Where, if $x(t) \geq \chi$,

$$A(t) = a_0$$

if $x(t) < \chi$,

$$A(t) = a_0 \cdot \sqrt{2/(\gamma-1)} \cdot \{(\gamma+1)/2\}^{(\gamma+1)/2(\gamma-1)} \cdot x_g^{-(\gamma+1)/2\gamma} \cdot \sqrt{x_g^{(\gamma-1)/\gamma} - 1}$$
$$c_g = c_{0g} \cdot \left(x_g/x_{0g}\right)^{(\gamma-1)/\gamma}$$

The mechanical response model consists of two parts:

1. Reduction of chamber volume due to thermal expansion of the "penetration thickness" $\sqrt{\mathrm{a} \cdot t}$ during a time interval δt:

$$\phi(t) = e^{-2\xi\sqrt{t}}$$
$$\delta V_{te} = -B \cdot \sqrt{t} \cdot \left(\Theta_{gi} - 1\right) \cdot (1-\phi) \cdot \delta t$$

2. Change in chamber volume during the interval δt due to pressure change:

$$\delta V_{pr}(t) = \Lambda \cdot \left(x_g - 1\right) \cdot \delta t$$

The net volume change over interval δt is:

$$\delta V(t) = \delta V_{te}(t) + \delta V_{pr}(t)$$

The chamber volume at time t is then:

$$V(t) = V(t - \delta t) + \delta V(t)$$

Heat loss modeling is as follows:
The thermal response of the chamber due to heat transfer at the walls can be modeled as being due (a) either to conduction only, or (b) due to both convection and conduction.

The temperature ratio change, $\delta\Theta_g(t)$, in the chamber during a time interval δt due to heat loss to the walls is calculated as follows:

$$\Theta_g^{av}(t) = \{\Theta_{gi}(t) + \Theta_g(t - \delta t)\}/2$$

For $t > 0$, if $\Theta_g^{av}(t) > \Theta_{cg}$,

(a) if it is assumed that heat loss is due to conduction only, then

$$\delta\Theta_g(t) = -\beta_0 \cdot [\{\delta t \cdot (\Theta_{gi} - 1)/2\sqrt{t}\} + (\Theta_{gi} - \Theta_g^{av}) \cdot \sqrt{t}]$$

(b) if the assumption of **Newtonian heating of the chamber walls with surface conductance (i.e. convection and conduction)** is made, then

$$\delta\Theta_g(t) = -\{\delta t \cdot \mathrm{u} \cdot AR_0/(\rho_g \cdot V \cdot C_p)\} \cdot (\Theta_g^{av} - 1) \cdot \phi$$

If $\Theta_g^{av}(t) \leq \Theta_{cg}$, or if $t \leq 0$,

$$\delta\Theta_g(t) = 0$$

The net temperature ratio change $\Delta\Theta_g$ due to heat loss up to time t is

$$\Delta\Theta_g(t) = \Delta\Theta_g(t - \delta t) + \delta\Theta_g(t)$$

The net temperature change as a fraction of the initial (maximum) temperature is:

$$D\Theta_g(t) = \Delta\Theta_g(t)/\Theta_0$$

The chamber and efflux variables, adjusted for mechanical and thermal response of the chamber, can be calculated as follows:

(a) the adjusted chamber pressure ratio x

$$x(t) = x_g \cdot \left[\{(V - \delta V_{pr})/V\}^{\gamma} \cdot \{max(\Theta_g + \delta\Theta_g, \Theta_{cg})/\Theta_g\}^{\gamma/(\gamma-1)}\right]$$

(b) the adjusted overpressure ratio Ox

$$Ox(t) = x(t) - 1$$

(c) the overpressure impulse ratio OI

$$OI(t) = OI(t - \delta t) + Ox \cdot \delta t$$

(d) the adjusted chamber density ratio R

$$R(t) = R_0 \cdot (x/x_{0g})^{1/\gamma}$$

(e) the adjusted critical density ρ_{cr}

$$\rho_{cr}(t) = \rho_{og} \cdot (R/R_0) \cdot \{2/(\gamma + 1)\}^{1/(\gamma-1)}$$

(f) the adjusted chamber temperature ratio Θ

$$\Theta(t) = \Theta_0 \cdot (x/x_{0g})^{(\gamma-1)/\gamma}$$

(g) the sound speed in the chamber c

$$c(t) = c_{og} \cdot \sqrt{\Theta}$$

(h) the critical sound speed c_{cr}

$$c_{cr}(t) = c \cdot \sqrt{2/(\gamma + 1)}$$

(i) the velocity of efflux U, the mass flow rate $\dot{m}$, and the efflux Mach number M:
if $x \geq \chi$,

$$U(t) = c_{cr}$$
$$\dot{m}(t) = a_0 \cdot \rho_{cr} \cdot U$$
$$M(t) = 1$$

if $x < \chi$,

$$\dot{m}(t) = a_0 \cdot \sqrt{(\gamma+1)/(\gamma-1)} \cdot \rho_{0a} \cdot R \cdot c_{cr} \left[x^{-2/\gamma} - x^{-(\gamma+1)/\gamma}\right]^{1/2}$$
$$U(t) = \dot{m}/(a_0 \cdot \rho_{cr})$$
$$M(t) = \sqrt{\{2/(\gamma-1)\} \cdot (x^{-1/\gamma} - 1)}$$

(j) the mass flow increment δm and the total mass outflow by time t

$$\delta m(t) = \dot{m} \cdot \delta t$$
$$m_{tot}(t) = m_{tot}(t - \delta t) + \delta m$$

APPENDIX B

LISTING OF THE CODE MATVENT

(With an Example Run)

```
%matvent.m
%_____________________________________________________________

%AN INTERNAL AIRBLAST CODE FOR VENTING FROM A RESPONDING
%OR NON-RESPONDING SINGLE CHAMBER.
%
%DEVELOPED BY —DEV S. SRINIVASA
%LOGICON RDA, 6053 W. CENTURY BLVD, LOS ANGELES, CA 90045
%PH: (310) 645-1122 ext 338; FAX(310) 645-2553
%_____________________________________________________________

%Set plotting indices as elements of a 1X5 matrix in which;
%element 1 is the index for overpressure and ovpr impulse ratio plots
%element 2 is the index for density and temperature ratio plots
%element 3 is the index for efflux velocity and Mach number plots
%element 4 is the index for mass flow rate and total efflux mass plots
%element 5 is the index for relative volume change and heat loss plots


kplt=input('plot indices as a 1x5 matrix');%for example,type[1 1 1 1 1],hit Enter


%The input values for the example are shown after %
MSIM=input('Mass of simulant,gms');% 16116
frac=input('Fraction fluidized');% 0.667
MC4=input('Mass of explosive, gms');% 0.95*453.6
ECON=input('Yield per gm of explosive,like 6.65e10 for C-4')% 6.65e10
W=MC4*ECON; %Explosion yield of 0.95 lbs C-4
Cst=input('Thermal capacity of chamber wall material,j/gm./deg K,like 0.449e7 for iron or steel');%0.449e7

kst=input('Thermal conductivity of wall material,ergs/cm.sec.K.,like 1.0e7 for steel');%1.0e7
lxpst=input('Coefft of linear expansion,cm/cm/ K,like 1.206e-5 for 1020 steel');%1.206e-5
rhost=input('Density of wall material,gms/cc,like 7.86 for 1020 steel');%7.86
%Note: Set usk to 0 for thermally non-responding case
usk=input('Convection coefft,ergs/sec.cm^2 K,like 1.419222e7 for steel') %1.419222e7
ast=kst/(rhost*Cst);%Thermal diffusivity of wall material,cm^2/sec
flm=usk/(rhost*Cst*kst)^0.5; %film coefficient
Cp = 1.03e7;  %1.03 joules/gm K (CRC Handbook),Sp. heat at con.pr for air
lc=input('Chamber length,width,depth as a 1x3 matrix, all in cms')%[173.99 130.81 49.53]
Arst=2.0*(lc(1,1)*lc(1,2)+lc(1,2)*lc(1,3)+lc(1,3)*lc(1,1)); %Wall area of chamber
V0=lc(1,1)*lc(1,2)*lc(1,3) %Initial chamber volume, cc
lhmd=6*V0/Arst;  %length scale for chamber (6*Vol/Area),cm
rhoza=0.001225  %Ambient air density,g/cc
rhozc=(rhoza*V0+MC4)/V0;  %initial density of chamber contents w/o beads
rhozt0=rhozc+(frac*MSIM/V0);  %Density of fluid plus fluidised material
area=input ('Area of vent opening,sq.cms');%31.66922
```

```
p0=1.01325e6;  %Reference pressure in dynes/sq.cm (=1 atm)
gam=input('Assumed gamma for chamber gases');%1.35
TEMR=298.15;  %Reference temperature 25 C
beta0=(Cst/Cp)*(rhost/rhozt0)*(Arst/V0)*sqrt(ast);
ss0=sqrt(gam*p0/rhozt0);  %Sound speed in ambient chamber gases at atm · pr ·
x0=1+((gam-1)*W/(V0*p0)); %Initial (Max) Pressure ratio
xcut=(1/x0)^((gam-1)/gam);%cutoff value for pressure
ssmax0=ss0*sqrt(x0);  %average initial sound speed in chamber
sscrit0=((2/(gam+1))^0.5)*ssmax0; %Initial critical speed of sound


%Note: set ssch to a very large value,say 1.e25, for non-responding case
ssch=input('Compressional wavespeed in wall material,cm/s,like 5.9436e5 for steel');  %5.9436e5
chimpd=rhost*ssch; %Chamber matl impedance gm/cm**2.sec
cndv=(Arst*p0/chimpd);  %constant in volume change adjustment to pressure
DR0=(rhozt0/rhoza);  %Max (initial) density ratio
DT0=gam*W/(Cp*rhozt0*V0); %Temp rise,assuming that all fluid mass in chmbr participates
TEM0=(DT0+TEMR);  %Initial temperature(deg K) of chamber after explosion
TR0=TEM0/TEMR;  %Initial temperature ratio
TRcut=xcut*TR0;
gchok=(0.5*(gam+1))^(gam/(gam-1));  %Choking pressure ratio.
rhozt0c=((2/(gam+1))^(1/(gam-1)))*rhozt0; %Critical density
if (x0 /gchok) > 1,
VEL0=sscrit0;  %Efflux velocity is same as critical sound speed
MSDOTE0=area*rhozt0c*VEL0; %Mass rate of flow
ME0=1;
elseif (x0 /gchok) < 1,
MSDOTE0=area*(((gam+1)/(gam-1))^0.5)*(rhozt0*(sscrit0*((x0^(-2/ga m))-(x0^(-(gam+1)/gam)))^0.5));

VEL0=MSDOTE0/(rhozt0c*area);
ME0=((2/(gam-1))*(x0^((gam-1)/gam)-1))^0.5;
else,
VEL0=sscrit0;  %Efflux velocity at choking point
MSDOTE0=area*rhozt0c*VEL0;
ME0=1;
end;


%Specify initial time,end time,tolerance,trace in 1X4 matrix


TMTOL=input('initial time,end time,tolerance,trace of calcn as 1X4 matrix');%[0 1 1.e-4 0]


t0=TMTOL(1,1);tfinal=TMTOL(1,2);tol=TMTOL(1,3);trace=TMTOL(1,4);


%Initialization

pow = 1/3;
```

```
t = t0;
hmax = (tfinal - t)/100;
hmin = (tfinal - t)/20000;
h = (tfinal - t)/100;
xx0=x0';DDR0=DR0';TTR0=TR0';VVEL0=VEL0';MME0=ME0';
x = x0(:); ox=x-1;
beta=beta0(:);
ssmax=ssmax0(:);
rhozt=rhozt0(:);
V = V0(:);
TR= TR0(:);
DR= DR0(:);
VEL=VEL0(:);
ME= ME0(:);
MSDOTE=MSDOTE0(:);
tout = t;
xout = x.'; len=length(xout);
oxout=ox.';


for i=1:len,
Tls0(i)=0;
DTls0(i)=0;
TTMS0(i)=0;
OI0(i)=0;
DV0(i)=0;
end;
Tls=Tls0(:);DTls=DTls0(:); TOTMASE=TTMS0(:);OI=OI0(:);DV=DV0(:);
DRout=DR.' ;
TRout=TR.' ;
VELout=VEL.';
MEout=ME.';
MSDout=MSDOTE.';
TOTMout=TOTMASE.';
OIout=OI.';
DVout=(DV./V0)';
DTout=(Tls./TR0)';


tau = tol * max(norm(x, 'inf'), 1);
if trace
clc, t, h, x
end


%The main loop

while (t < tfinal) & (h >= hmin)
if t + h > tfinal,
```

```
h = tfinal - t;
end
TRB=TR;

%Compute the slopes, using the Runge-Kutta Fehlberg integration scheme

s1 = feval('intair8', t, x, V,xx0,ssmax,area,TR,TRcut,gam); s1 = s1(:);
s2 = feval('intair8', t+h, x+h*s1, V,xx0,ssmax,area,TR,TRcut,gam); s2 = s2(:);
s3 = feval('intair8', t+h/2, x+h*(s1+s2)/4, V,xx0,ssmax,area,TR,TRcut,gam); s3 = s3(:);

%Estimate the error and the acccptable error

delta = norm(h*(s1 - 2*s3 + s2)/3,'inf');
tau = tol*max(norm(x,'inf'),1.0);

%Update the solution only if the error is acccptable

if delta < = tau
t = t + h;
x = x + h*(s1 + 4*s3 + s2)/6;

%Reduction of Chamber volume due to thermal expansion of pentrn thckness

dvtcon=Arst*lxpst*sqrt(ast)*TEMR; ex=exp(-2*flm*sqrt(t));
dvt=-dvtcon*h*(t^0.5)*(TR-1)*(1-ex);

%pressure adjustment for volume change during timestep h

V=V +h*cndv*(x-1)+dvt; VR=(V/V0); DV=(V-V0)./V0;

%Temp change in chamber during time increment h due to heat loss

TRAVG=0.5*(TR+TRB);
if t > 0.0,
if TRAVG > TRcut,

% Newtonian heating only of chamber wall,with surface conductance
```

```
DTls=-h*(usk*Arst/(rhozt*V*Cp))*(TRAVG-1)*exp(-2*flm*t^0.5);
elseif TRAVG<TRcut,
DTls=0;
else,
DTls=0;
end;
elseif t < 0.0,
DTls=0.0;
else,
DTls=0.0;
end;
Tls=Tls+DTls;
DTl=Tls./TR0;

%Adjusted pressure ratio

x=real(x*((((V-h*cndv*(x-1))/V)^gam)*(((max(TR+DTls,TRcut))/TR)^( gam/(gam-1)))));

%Adjusted density ratio

DR= real(DDR0*((x/xx0)^(1/gam)));

%Adjusted temperature ratio

TR=real(TTR0*((x/xx0)^((gam-1)/gam)));

%sound speed in the chamber

ssmax=real(ssmax0*(x*DDR0/(xx0*DR))^0.5);

% "critical" speed of sound;

sscrit = (sqrt(2/(gam+1)))*ssmax;

%Overpressure ratio

ox=x-1;

%Overpressure impulse ratio
```

```
OI=OI+ox*h;

%Critical density at updated time

rhoztc=rhozt0*((2/(gam+1))^(1/(gam-1)))*(DR/DDR0);

%Velocity and Mass flow rate

if x > gchok,
VEL=sscrit;   %Efflux velocity is same as critical sound speed
MSDOTE=area*rhoztc*VEL; %Mass rate of flow
ME=1;
elseif x < gchok,
MSDOTE=real(area*(((gam+1)/(gam-1))^0.5)*rhoza*(DR*(sscrit*(x^(-2 /gam)-x^(-(gam+1)/gam))^0.5))

VEL=MSDOTE/(rhoztc*area);
ME=real(((2/(gam-1))*((x)^((gam-1)/gam)-1))^0.5);
else,
VEL=sscrit; % Efflux velocity at choking point
MSDOTE=area*rhoztc*VEL;
ME=1;
end;

%Mass flow increment

DMSE = MSDOTE*h;

%Mass outflow upto time t

TOTMASE=TOTMASE +DMSE;

%store vent times and total mass vented

if ox > = 0.01
Vtm=t; Tmvtd=TOTMASE;
end;

tout = [tout; t];
xout = [xout; x.'];
oxout= [oxout;ox.'];
```

```
OIout=[OIout;OI.'];
DRout= [DRout; DR.'];
TRout= [TRout; TR.'];
VELout=[VELout; VEL'];
MEout= [MEout; ME.'];
MSDout=[MSDout;MSDOTE.'];
TOTMout=[TOTMout;TOTMASE.'];
DVout=[DVout;DV.'];
DTout=[DTout;DTI.'];
end %end of the 'if delta < tau' loop


if trace
home, t, h, x
end


%Update the step size


if delta ~ = 0.0
h = min(hmax, 0.9*h*(tau/delta)^pow);
end
end;      %end of the main('while') loop


if (t < tfinal)
disp('SINGULARITY LIKELY.')
t
end


end;


%Display the venting duration and total mass vented on the screen


disp('Vent time(sec) Total vented mass(gm)')
[Vtm Tmvtd]


%form strings for placement on plot


st1='Duration of Venting =' ;st2=num2str(Vtm); st3=' sec';
st4='Total Vented Mass =';st5=num2str(Tmvtd); st6=' gms';
str1=[st1 st2 st3];str2=[st4 st5 st6];
```

```
%PLOT THE OUTPUT TIME HISTORIES
%Note: The gtext(' ') items are for placement with the mouse

if kplt(1,1) > 0,
plotyy(tout,oxout,tout,OIout,'Overpressure Impulse Ratio');grid;
title('EXAMPLE FIG 1: BLAST VENTING- OVERPRESSURE AND IMPULSE HISTORIES')
xlabel('Time, sec')
ylabel('Overpressure Ratio')
gtext('Overpressure');
gtext('Ovp Impulse');
pause;
figure
else,
disp('No Overpressure or Overpressure Impulse plots')
end;


if kplt(1,2) > 0,
plotyy(tout,DRout,tout,TRout,'Temperature Ratio');grid;
title('EXAMPLE FIG 2: DENSITY RATIO AND TEMPERATURE RATIO HISTORIES')
xlabel('Time, sec')
ylabel('Density Ratio')
gtext('Density');
gtext('Temperature');
pause;
figure
else,
disp('No Density Ratio or Temperature Ratio plots')
end;


if kplt(1,3) > 0,
plotyy(tout,VELout,tout,MEout,'Mach Number of Efflux');grid;
title('EXAMPLE FIG 3: EFFLUX VELOCITY AND MACH NUMBER HISTORIES ')
xlabel('Time, sec')
ylabel('Efflux Velocity, cm/sec')
gtext('Velocity');
gtext('Mach No');
pause;
figure
else,
disp('No Efflux Velocity or Mach Number plots')
end;


if kplt(1,4) > 0,
plotyy(tout,MSDout,tout,TOTMout,'Total Efflux Mass, gms');grid;
title('EXAMPLE FIG 4: EFFLUX MASS FLOW RATE AND TOTAL MASS HISTORIES')
```

```
xlabel('Time, sec')
ylabel('Mass flow rate, gm/sec')
gtext('Mass rate');
gtext('Total Mass');
gtext(str1);%Prints Venting Duration
gtext(str2);%Prints Total Mass vented
pause;
figure
else,
disp('No Mass Flow Rate or Total Efflux Mass plots')
end;


if kplt(1,5) > 0,
plotyy(tout,DVout,tout,-DTout,'Relative Heat Loss');grid;
title('EXAMPLE FIG 5: RELATIVE VOLUME CHANGE AND HEAT LOSS HISTORIES');
xlabel('Time, sec')
ylabel('Relative Volume Change')
gtext('Volume Change')
gtext('Heat Loss')
pause;
else,
disp('No Relative Volume Change or Relative Heat Loss plots')
end;


function xp=intair8(t,x,V,xx0,ssmax,area,TR,TRcut,gam)
%_____________________________________________________________________

gm=gam;gl=gm-1.0;g2=0.5*(gm+1.0)/gm; g3=0.5*gl/gm;
g3r=0.5/g3;g4=-1.0/gm;gchok=(gm*g2)^g3r;
gch1=((g2*gm)^(-g2*g3r))*((0.5*gl)^0.5);
%_____________________________________________________________________

%It is assumed that initially, the pressure rise due to explosion in
%the chamber is instantaneous;
%_____________________________________________________________________

%Choked flow


if (x/gchok) > 1,
AR=area;


%No choking
elseif (x/gchok) < 1,


AR=area*((g2*gm)^(g2*gm/gl))*((2/gl)^0.5)*(x^(-g2))*((x^ (2*g3)-1.0)^0.5);
else,
```

```
AR=area;
end;
xssmx=(xx0^(-g3))*ssmax;


%Time derivative of chamber pressure


if TR>TRcut
xp=-gm*((g2*gm)^(-g2*gm/gl))*(xssmx*(AR/V))*(x^(1+g3));
elseif TR<TRcut,
xp=0;
else,
xp=0;
end;
```

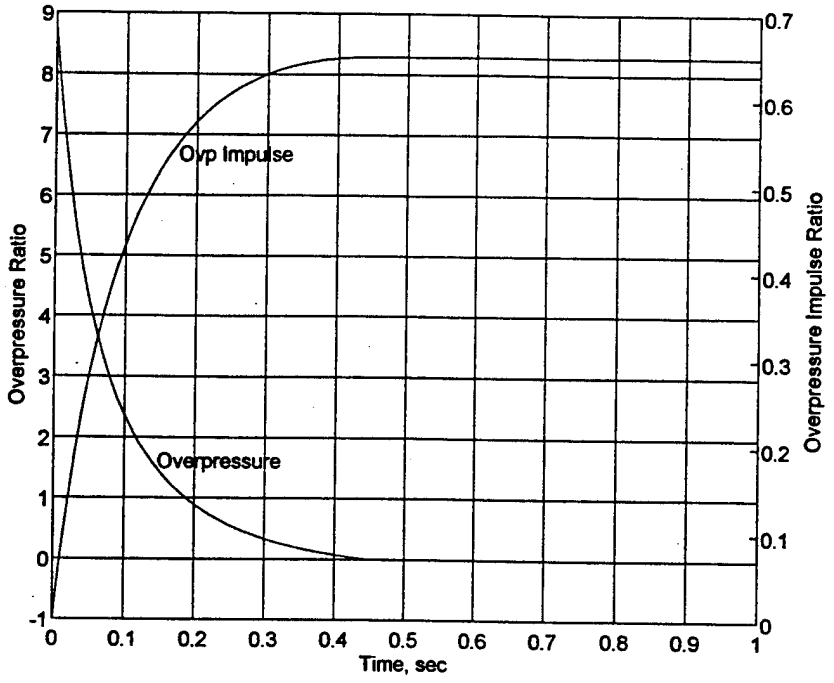

Figure B-1. Blast venting — overpressure and overpressure impulse histories.

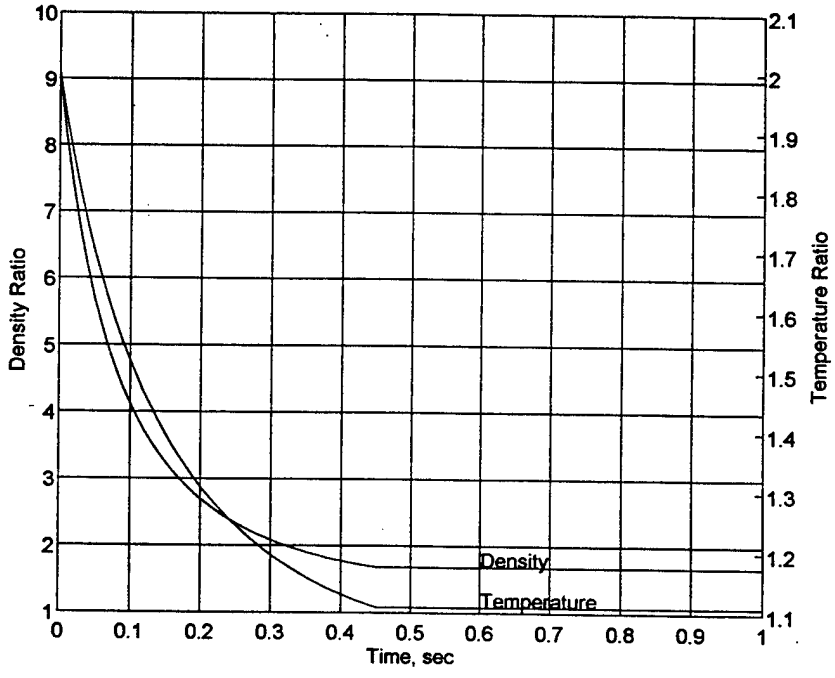

Figure B-2. Density ratio and temperature ratio histories.

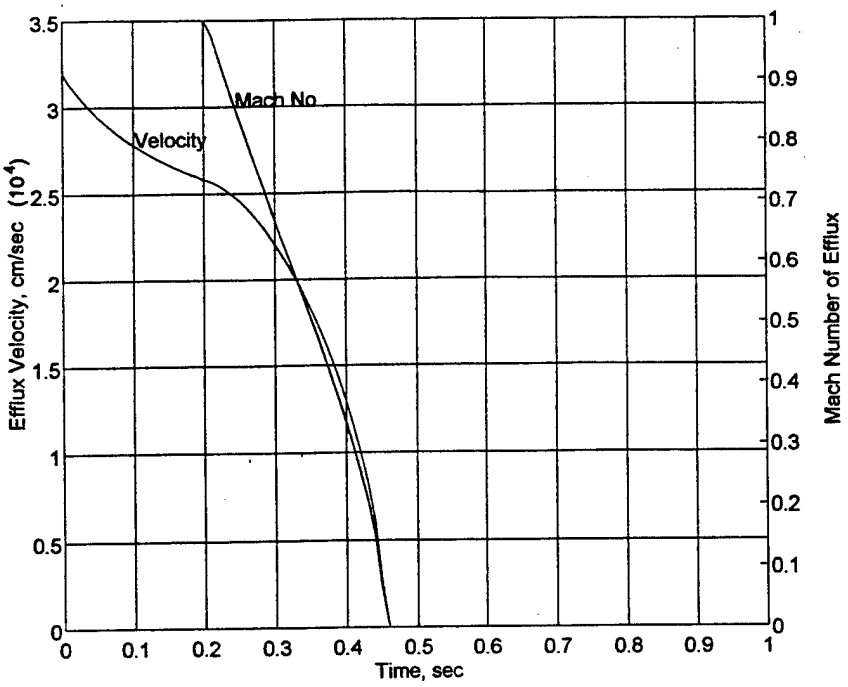

Figure B-3. Efflux velocity and mach number histories.

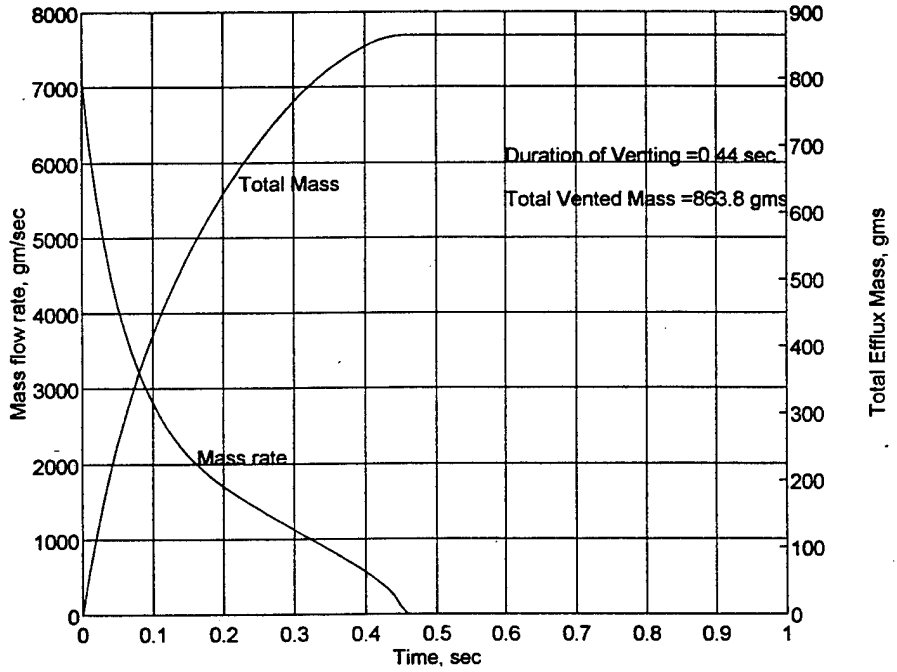

Figure B-4. Mass flow rate and total efflux mass histories.

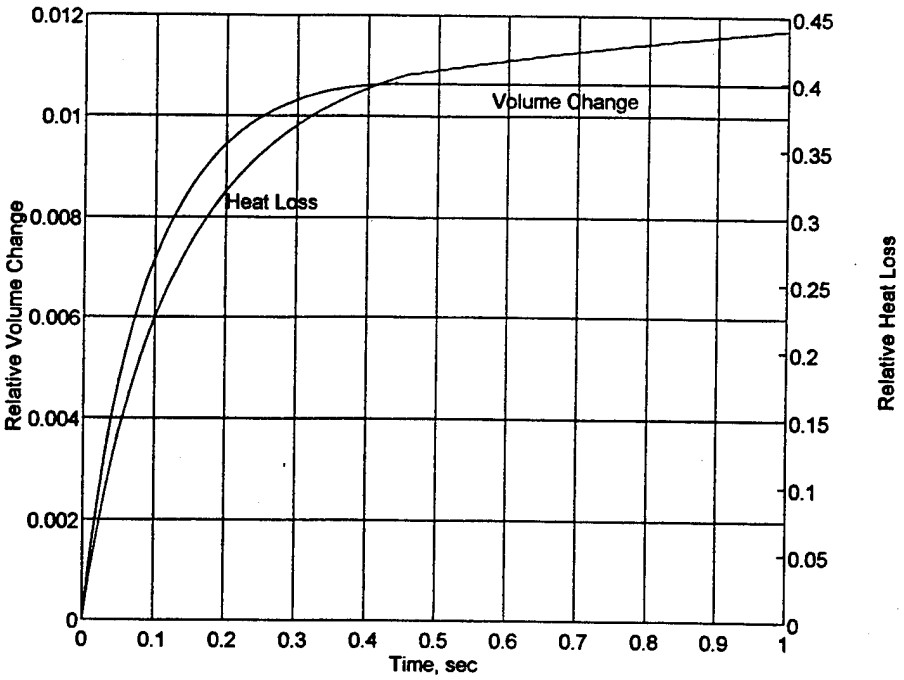

Figure B-5. Relative volume change and relative heat loss histories.

APPENDIX C

LIST OF SYMBOLS

Roman symbols

a = Thermal diffusivity of wall material

a_0 = Vent cross-sectional area

AR_0 = Initial area of chamber wall surface

B = A constant in computing volume change due to thermal expansion

c_w = Compressional wave speed in wall material

c_{0ag} = A reference sound speed

c_{0g} = Initial (maximum) sound speed in chamber

c_{0cr} = Initial critical sound speed

C = Specific heat of the wall material of chamber

C_p = Specific heat of air at constant pressure

f = Fraction of simulant fluidized

$\dot{m}_0$ = Initial (maximum) Mass Rate of Efflux

M_0 = Initial Mach Number of Efflux

M_{ex} = Mass of explosive

M_{hm} = Mass of loose hazardous material simulant inside the chamber

Q = Gain (or loss) of heat energy

$\dot{Q}$ = Heat flow rate

δQ = Increment in gain or loss of heat energy

p_0 = Initial (maximum) pressure of chamber gases

p_{0a} = Reference (ambient) pressure (= 1.01325*10^6 dynes/sq. cm)

$p_g(t)$ = Quasistatic pressure in the chamber at time t

R_0 = Initial (maximum) density ratio (= ρ_{og}/ρ_{oa})

t = Time after explosion

δt = Time increment

T_0 = Initial (maximum) temperature of chamber gases

T_{0a} = Reference (ambient) temperature (a constant, e.g. 298.15° K)

$T_g(t)$ = Quasi-static temperature of chamber gases at time t

u = Convection coefficient for wall material and chamber gases

U_0 = Initial (maximum) efflux velocity through vent

V_0 = Initial volume of chamber

w = Impedance of wall material

W = Yield of explosion

x_{0g} = Initial (maximum) pressure ratio in chamber

x_{cg} = Cutoff for pressure ratio

$x_g(t)$ = Normalized quasi-static pressure

Greek symbols

β_0 = Constant in heat loss by conduction

χ = Choking pressure ratio

ϵ = Coefficient of linear expansion of wall material

γ = Specific heat ratio for chamber gases (a constant, e.g. 1.35)

κ = Thermal Conductivity of wall material of chamber

Λ = Constant in volume change adjustment to pressure

ρ_{0a} = Ambient air density

ρ_{0c} = Initial density of chamber contents without simulant

ρ_{0cr} = Critical density

ρ_{0g} = Initial density of chamber gases including fluidized simulant

$\rho_g(t)$ = Density of chamber gases at time t

ρ_w = Density of wall material of chamber

Θ_0 = Initial (maximum) temperature ratio in chamber

Θ_{cg} = Cutoff for temperature ratio

$\Theta_g(t)$ = Temperature ratio

$\Theta_{gi}(t)$ = Interim temperature ratio ξ = Film coefficient

DISTRIBUTION LIST

DNA-TR-94-178

DEPARTMENT OF DEFENSE

DEFENSE NUCLEAR AGENCY
2 CY ATTN: ISST
ATTN: SPWE LTC JIM HODGE
ATTN: SPWE LTC MARK BYERS
ATTN: SPWE R COX
ATTN: WEL DAVE MYERS
ATTN: WEL L WITTWER
ATTN: WEP G ULLRICH

DEFENSE TECHNICAL INFORMATION CENTER
2 CY ATTN: DTIC/OCP

DEPARTMENT OF THE ARMY

U S ARMY RESEARCH LAB
ATTN: SLCBR-TBD G ROECKER

DEPARTMENT OF THE NAVY

NAVAL RESEARCH LABORATORY
ATTN: CODE 6795 DR MANKA

DEPARTMENT OF DEFENSE CONTRACTORS

INFORMATION SCIENCE INC
ATTN: W DUDZIAK

KAMAN SCIENCES CORPORATION
ATTN: DASIAC

LOGICON R & D ASSOCIATES
ATTN: D GAKENHEIMER
2 CY ATTN: D SRINIVASA

LOGICON R & D ASSOCIATES
ATTN: BOB DEBELL
ATTN: RITA COOPER
ATTN: TOM MAZZOLA

LOGICON R & D ASSOCIATES
ATTN: G GANONG

MAXWELL LABORATORIES INC
ATTN: T PIERCE

MAXWELL LABORATORIES INC
ATTN: C NEEDHAM

SCIENCE APPLICATIONS INTL CORP
ATTN: J SIMMONS